ELSEVIER

Journal of Structural Geology 29 (2007) 562–582

JOURNAL OF STRUCTURAL GEOLOGY

www.elsevier.com/locate/jsg

Characteristics of a kilometer-scale high strain zone in the lower continental crust: Mt. Hay block, central Australia

C. Waters-Tormey [a,*], B. Tikoff [b]

[a] *Department of Geosciences and Natural Resources Conservation and Management, Western Carolina University, 349 Stillwell Building, Cullowhee, NC 28723, USA*

[b] *Department of Geology and Geophysics, University of Wisconsin, Madison, WI 53706, USA*

Received 8 July 2005; received in revised form 28 October 2006; accepted 30 October 2006
Available online 2 January 2007

Abstract

A granulite facies high strain zone was studied on Capricorn Ridge, part of the Mt. Hay block granulites in the Arunta inlier, central Australia. Deformation occurred in these primarily mafic composition granulites at lower crustal conditions (~8 kb, ~800 °C) at 1740–1690 Ma. Pervasive and consistently oriented foliation (striking SSW and dipping steeply) and lineations (pitching steeply eastward) occur within the shear zone. The high strain zone is recognized by the presence of SL-tectonites, parallelism of grain shape fabrics and lithologic boundaries, transposition of lithologic boundaries into parallelism with the foliation, and the local occurrence of sheath-like folds. Field-based fabric mapping uses compositional foliation intensity as a proxy for finite strain to document strain variations within the Capricorn Ridge high strain zone. There is no observed microstructural grain size reduction that corresponds to these strain variations. Fabric intensity increases from the centers of the major lithologic units towards the contacts. 100 m-scale strain localization within Capricorn ridge occurs adjacent to major lithologic contacts, indicating competency contrast during lower crustal deformation.

Keywords: Granulite; Australia; Arunta; Strain localization; Lower crust; Competency

1. Introduction

Strain localization occurs within natural deformation zones irrespective of the style or kinematics of deformation (e.g., Gapais et al., 1987; Brown and Solar, 1998; Jin et al., 1998; Burg, 1999; Rutter, 1999; Tikoff and Goodwin, 2002; Arbaret and Burg, 2003; Crider and Peacock, 2004). The causes/mechanisms of internal strain localization therefore seem to be a first-order mechanical characteristic of the larger deforming zone. Understanding strain localization at relatively high homologous temperatures in naturally deformed ductile crust is critical information needed for lithosphere-scale rheological models.

Studies of natural deformation at relatively high homologous temperatures have documented several causes of strain localization. Many mechanisms involve the segregation of strain into weak phase domains such as fine grained domains (e.g., Behrmann and Mainprice, 1987; Altenberger, 1997; Kruse and Stunitz, 1999), compositional domains deforming at higher strain rates (e.g., Altenberger, 1997; Lonka et al., 1998; Martelat et al., 1999; Hippertt et al., 2001), partially molten zones (e.g., Brown and Solar, 1998; Snoke et al., 1999), and subsolidous syntectonic intrusives (Hanmer, 1997). Changes in external deformation conditions also drive strain localization. For example, syndeformational changes in temperature can activate or deactivate grain scale mechanisms (e.g., Hanmer, 1997; Lister and Dornsiepen, 1982; Mainprice et al., 1986; Stipp et al., 2002; Rosenberg and Stunitz, 2003), metamorphic reactions can generate new fine-grained phases (e.g., Watts and Williams, 1983; Kruse and Stunitz, 1999; Newman et al., 1999; Williams et al.,

* Corresponding author. Tel.: +1 828 227 3696; fax: +1 828 227 7393.
E-mail address: cherylwt@wcu.edu (C. Waters-Tormey).

0191-8141/$ - see front matter © 2006 Elsevier Ltd. All rights reserved.
doi:10.1016/j.jsg.2006.10.011

2000; Handy and Stunitz, 2002), and chemical disequilibrium can accelerate dynamic recrystallization (e.g., Williams et al., 2000; Rosenberg and Stunitz, 2003). Further, critical volumes of partial melt can initiate shear instabilities (e.g., Brown and Solar, 1998; Snoke et al., 1999), cataclasis (e.g., Brown and Solar, 1998), and make diffusional deformation mechanisms more efficient (Paterson, 1995). Cataclasis due to either overpressuring of a syntectonic fluid phase or episodic high strain rates can produce a fine grained phase (e.g., Austrheim, 1987; Vissers et al., 1997). As is the case at higher levels of the crust, the sites of strain localization can also be controlled by the tendency to reactivate pre-existing structures (e.g., Hanmer, 1997).

At present, it is unclear what the common causes of strain localization are in the lower crust. Theoretical models have examined mechanical properties of ductilely deforming zones with mixed weak and strong phases and generally conclude that strain will localize in an interconnected weak phase (e.g., Olgaard, 1990; Handy, 1994). Many models focusing on bulk mechanical properties of the lithosphere assume that grain scale deformation mechanisms in interconnected quartz- or feldspar-rich domains make these the weak phases controlling deformation in the lower crust (e.g., White and Breton, 1985; Carter and Tsenn, 1987; Scholz, 1988; Molnar, 1992; Kohlstedt et al., 1995; Benes and Davy, 1996; Gartrell, 2001). Yet, there are relatively few studies of naturally deformed lower crust that test this assumption. This contrasts with the relatively larger body of work examining the common causes of strain localization in natural deformation in upper crustal (e.g., Miller et al., 1983; Chester and Logan, 1986; Evans, 1988; Lloyd and Knipe, 1992; Agar, 1994; Goodwin and Wenk, 1995; Tsurumi et al., 2003; Whitmeyer and Simpson, 2003), mid-crustal (e.g., Berthé et al., 1979; Burg et al., 1981; Law et al., 1984; Simpson, 1985; Ghosh and Sengupta, 1987; Lloyd et al., 1992; Dunlap et al., 1997; Dutruge and Burg, 1997; Whitmeyer and Simpson, 2003), and mantle (e.g., Drury et al., 1991; Jaroslow et al., 1996; Vissers et al., 1997) settings.

In this paper, we present preliminary results from the first structural study of a Paleoproterozoic, km-scale, lower-crustal high strain zone exposed in the Mt. Hay block, central Australia (Fig. 1). Deformation of the Mt. Hay granulites occurred at ~800 °C and ~8 kb during the 1740–1690 Ma Strangways event, formerly the late Strangways event of Collins and Shaw (1995) (Claoue-Long and Hoatson, 2005; Waters-Tormey et al., *in review*). Since the Mt. Hay block granulites lack strain markers, we primarily use relative fabric intensity as a proxy for relative finite strain intensity. In comparison with other structural domains in the Mt. Hay block, the northern edge – Capricorn ridge – is the highest strain zone. Given its >6 km thickness, Capricorn ridge would have been a significant zone of strain localization in the lower crust during the (late) Strangways event.

In order to study strain localization within Capricorn ridge, we take advantage of almost continuous exposure to examine meso- and macroscale field relationships. Fabric intensity gradients are defined by the shape and planarity of m-scale to cm-scale compositional domains. A fabric intensity map shows that compositional foliation intensifies across-strike towards major lithologic boundaries. If relative fabric intensity is interpreted in terms of relative strain intensity, the map-scale patterns identify 100 m thick strain localization zones straddling the major lithologic boundaries. We infer that strain localization adjacent to the major lithologic interfaces resulted from contrast in mechanical behavior between major lithologic domains during granulite facies deformation. The fabric mapping method provides a means of characterizing strain patterns even in the absence of distinct microstructural gradients or finite strain markers. Further, this study provides both evidence for a type of strain localization not documented in crustal rocks deformed at lower temperatures, and insight into mechanical heterogeneity during lower crustal deformation.

2. Geological setting

The Mt. Hay block is part of an ~160×50 km^2, east-west trending belt of granulites within the Arunta inlier of central Australia (Fig. 1; Shaw et al., 1984). The majority of the granulite protoliths formed as part of a Paleoproterozoic to Mesoproterozoic continental magmatic arc on the southern margin of the Northern Australia Craton, prior to assembly of the Proterozoic Australian terranes (Collins and Shaw, 1995; Young et al., 1995; Zhao and Bennett, 1995; Myers et al., 1996). The rest of the Arunta inlier is primarily composed of amphibolite facies metamorphic complexes and intrusives. Sediments of Neoproterozoic to Paleozoic intracontinental basins overlie the margins of the Arunta inlier on all sides (Shaw et al., 1991).

Granulites in the Mt. Hay block record peak metamorphic pressures and temperatures of ~8–9 kb and ~800–900 °C (Glikson, 1984; Warren and Shaw, 1995; Bonnay, 2001). Using recent geochronology data, granulite facies deformation, metamorphism and felsic magmatism events have been subdivided into a 1790–1770 Ma Yambah event and a 1740–1690 Ma Strangways event (Claoue-Long and Hoatson, 2005). These events are the only regional Proterozoic granulite facies deformation events recorded in the Arunta inlier (e.g., Watt, 1992; Ballevre et al., 1997). Two granulite facies deformation events are also recorded in the Mt. Hay block. Waters-Tormey et al. (*in review*) have correlated the earlier penetrative granulite facies, N-vergent, deformation with the Yambah event, and the overprinting, S-side up, granulite facies deformation in the Capricorn ridge shear zone with the Strangways event (Fig. 1). The restored orientation of the Capricorn ridge shear zone indicates an oblique divergent tectonic setting, which is consistent with the interpretation of regional magmatic activity (Zhao and McCulloch, 1995; Hoatson et al., 2005).

The Arunta granulites lie structurally above the Redbank Deformed Zone (RBDZ), a S-vergent thrust belt (Fig. 1b; e.g., Collins and Teyssier, 1989). The RBDZ probably originated as a Mesoproterozoic suture when the southern and northern parts of the Arunta terrane were juxtaposed (Shaw and Black, 1991; Myers et al., 1996). The RBDZ was reactivated during the Mesoproterozoic Anmatjira and Devonian Alice Springs events (e.g., Allen and Stubbs, 1982; Shaw

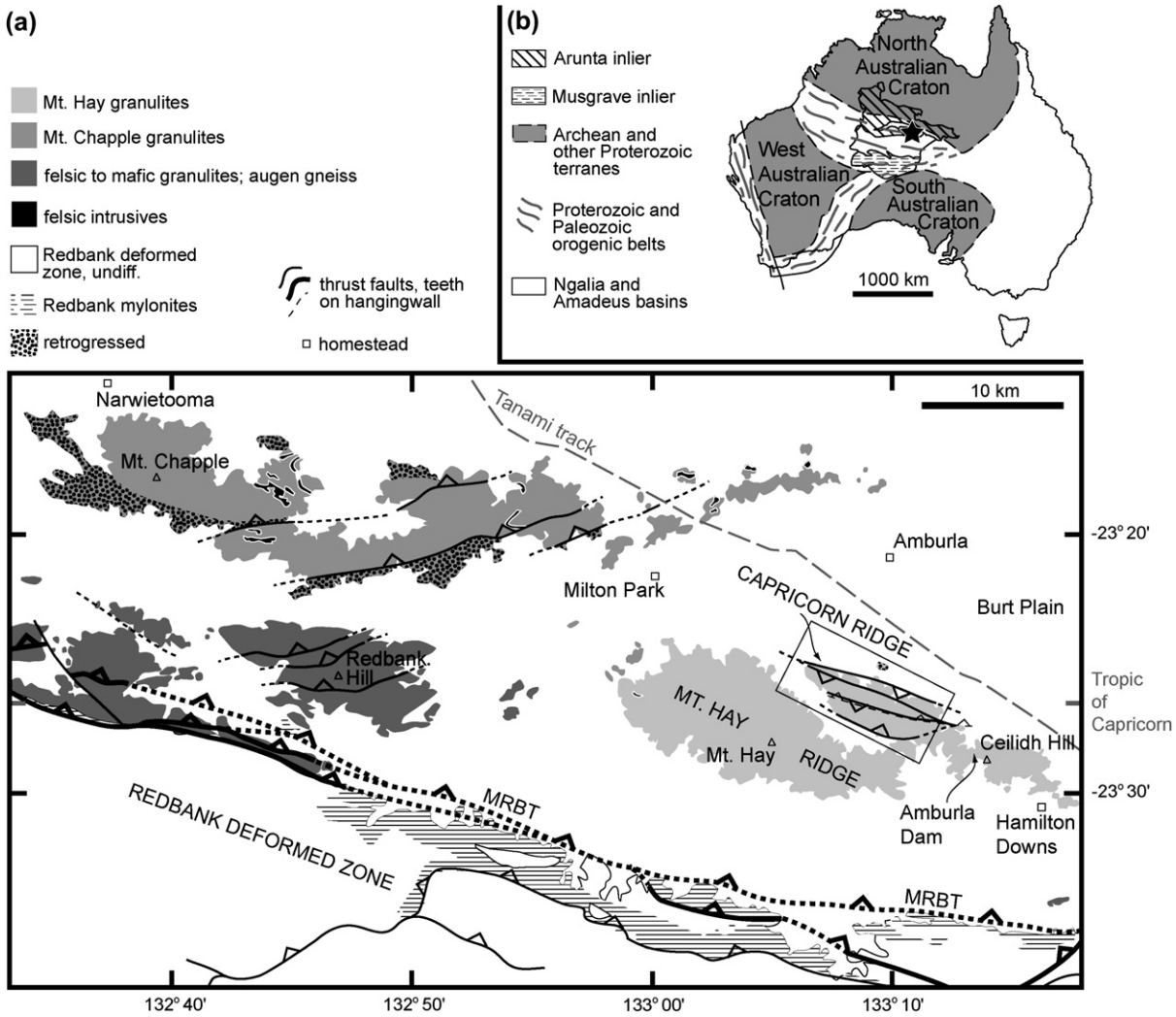

Fig. 1. (a) Generalized geologic map of study region (primarily after Warren and Shaw, 1995; also Teyssier, 1985; Teyssier et al., 1988; Shaw and Black, 1991; our mapping). The study area is the Mt. Hay block, approximately 80 km northwest of Alice Springs in the Northern Territory. Box shows location of Fig. 2. Teyssier (1985) focused on the Amburla dam area and southeastern Mt. Hay ridge. Detailed mapping by Bonnay (2001) was conducted on north-northwestern Mt. Hay ridge. (b) Archean and Proterozoic cratons, including Proterozoic Arunta and Musgrave inliers in Australia (after Myers et al., 1996; Van der Hilst et al., 1998; Wellman, 1988). The study area (star) is located within the Arunta inlier. Basins north (Ngalia) and south (Amadeus) of the Arunta inlier are remnants of the Neoproterozoic intracratonic superbasin in central Australia. Heavy grey lines indicate Archean and Proterozoic orogenic belts, locally reactivated in the Paleozoic.

and Black, 1991; Dunlap and Teyssier, 1995). Amphibolite and greenschist facies mylonitic reverse and thrust faults related to these events crosscut the lower crustal fabrics within the RBDZ and the granulites to the north (Figs. 1b and 2; Shaw and Black, 1991; Dunlap and Teyssier, 1995; Warren and Shaw, 1995; Waters-Tormey et al., *in review*). Gravity and reflection seismic data indicate that the main Redbank thrust roots into and vertically offsets the crust-mantle boundary by 25 km, and that reflectors from within the Mt. Hay granulites are subparallel with the crust-mantle boundary (Goleby et al., 1990; Korsch et al., 1998).

Uplift of the northern Arunta granulites primarily occurred during the S-vergent Alice Springs event (Dunlap and Teyssier, 1995; Biermeier et al., 2003). Shear zones associated with the Alice Springs orogeny probably enclose the Mt. Hay block structurally above and below, and separate it from granulite blocks to the west and the east (e.g., Teyssier et al., 1988; Shaw and Black, 1991).

2.1. The Mt. Hay block

The Mt. Hay block consists of three geomorphologically distinct domains (Fig. 1b): Mt. Hay ridge, Capricorn Ridge, and Ceidilh Hill (pronounced ‘‘kay-lee’’). Capricorn ridge (named informally because it lies on the Tropic of Capricorn) is a four km-wide exposure on the NE side of the Mt Hay block (Fig. 2). Mt. Hay granulites have gabbroic (intermediate) to pyroxenitic bulk compositions, in addition to lesser amounts of anorthositic, quartzofeldspathic, and rare garnet-quartzite, hornblendite, calc-silicate, and pelitic compositions. Pyroxenitic granulite always occurs with quartzofeldspathic granulite (up to ~40% by volume), so together these will be referred

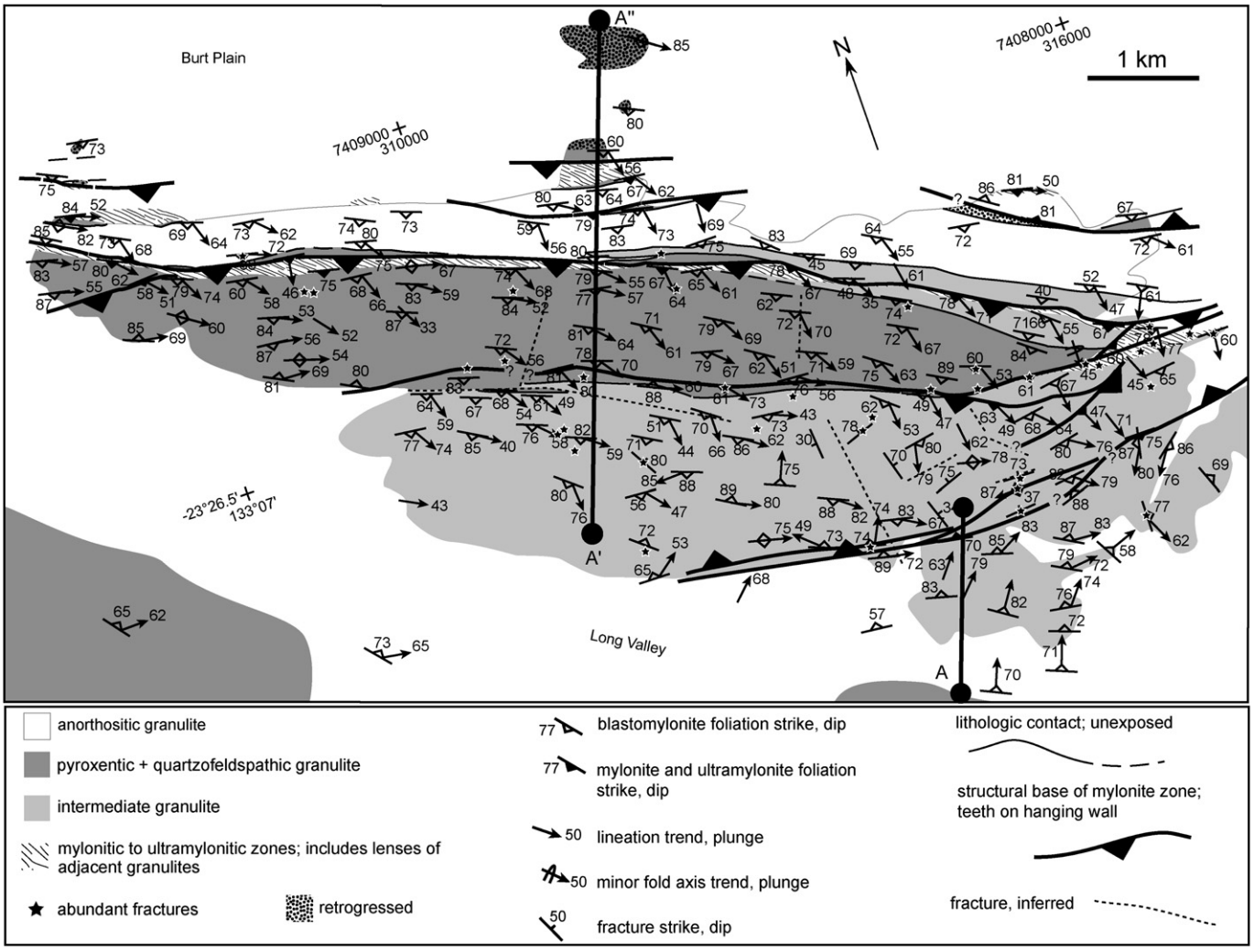

Fig. 2. Generalized geologic map of Capricorn ridge on the northeastern side of the Mt. Hay block. Location shown in Fig. 1. Thicker mylonite-ultramylonite zones containing m- to dm-scale lenses of the adjacent granulites (undifferentiated) are indicated; otherwise, mylonite outcrops are <5 m thick. Cross-section A-A′-A″ is shown in Fig. 13. Universal Transverse Mercator coordinates from grid 53K.

to as the pyroxenitic + quartzofeldspathic granulite unit (Figs. 2 and 3). This unit is the most abundant lithologic assemblage in the Mt. Hay block, comprising >70% of Mt. Hay ridge and Ceidilh Hill (Warren and Shaw, 1995). Metamorphosed sedimentary rocks are restricted to the NW fringes of Mt. Hay ridge (Glikson, 1984; Watt, 1992; Bonnay, 2001).

Geochemical analyses and U-Pb zircon geochronology suggest that the majority of the Mt. Hay granulites have igneous protoliths that were generated from a similar magmatic source (Warren and Shaw, 1995; Bonnay, 2001; Hoatson et al., 2005). The oldest protoliths were mafic intrusives that formed ~1803 Ma (Claoue-Long and Hoatson, 2005). The youngest protoliths are felsic intrusives that formed during minor magmatism at ~1770 Ma (Bonnay et al., 2000). Other protoliths include volcaniclastic sediments (Warren and Shaw, 1995).

The Mt. Hay granulites exhibit abundant evidence of ductile deformation. In thin section, grains of feldspar, quartz, and rarely pyroxene, are internally deformed as recorded by deformation twins (plagioclase) and undulose to patchy extinction. The granulite facies minerals all contribute to the grain shape fabric that helps to define foliation and lineation. Stretching parallel to the lineation is also indicated by local boudinage, sheath folds, and fold axes. Lineations sweep from NE-plunging in Mt. Hay ridge to SSE-SE plunging in Capricorn ridge (Figs. 2 and 4) and Ceidilh Hill on the northeast side of the Mt. Hay block. Foliations sweep from mostly NE-dipping in Mt. Hay ridge to SSW-dipping in Capricorn ridge (Fig. 4) and Ceidilh Hill. An S > L fabric (foliation better developed than lineation) and S-side-up shear sense in the Capricorn ridge shear zone distinguishes it from the rest of the Mt. Hay block.

Field relationships indicate that granulite facies deformation in the Mt. Hay block occurred in the solid state after the latest episode of magmatism (Glikson, 1984; Teyssier, 1985; Watt, 1992; this study). Although some quartzofeldspathic domains potentially had an anatectic origin (Bonnay, 2001), the lack of restitic melanosomes indicates that they do not represent *in situ* partial melting (Watt, 1992; this study).

The youngest stage of magmatism at ~1770 Ma is recorded by minor tonalitic stringers and blebs, and charnockitic

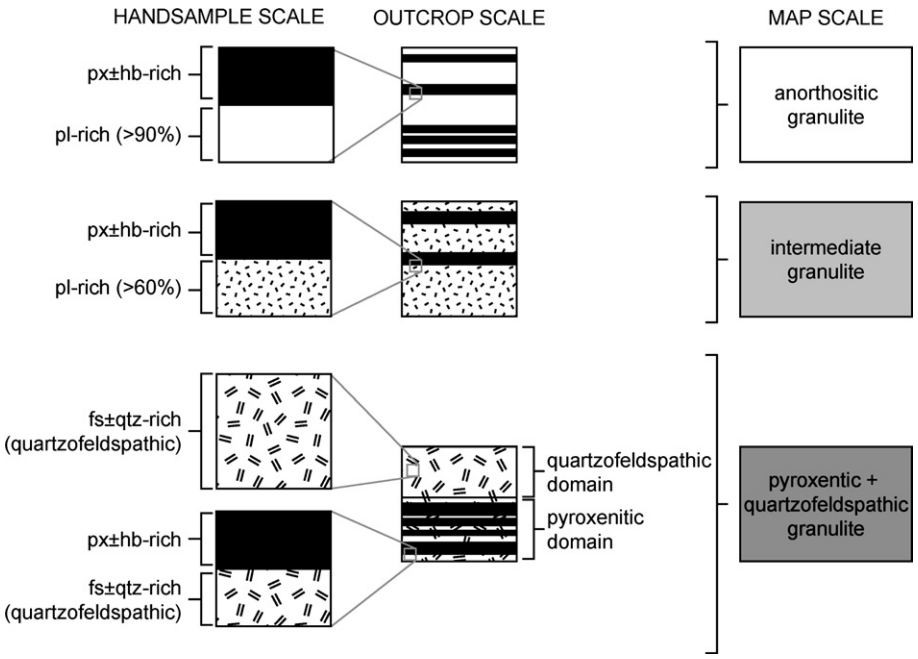

Fig. 3. Schematic illustration of lithologic heterogeneity at the outcrop, handsample, and map scales. Map scale lithologic units as in Fig. 2. Fabric (lineation and foliation) is homogenous within compositional domains at the handsample and outcrop scales. Fabric is heterogeneous at the 100 m-scale within the major lithologic units (anorthositic, pyroxenitic + quartzofeldspathic, intermediate granulites). For simplicity, the compositional domains are shown as layers representing strongest foliation intensity (Figs. 5–7).

intrusives (Bonnay, 2001), which are now recrystallized and form part of the mesoscale fabric. Leucosomes are found only in the pyroxenitic granulite and not in the other major lithologic bodies, suggesting that the deformation that juxtaposed the major lithologic bodies followed the youngest magmatism. Pyroxene and garnet porphyroclasts are often enclosed by quartzofeldspathic envelopes that taper to points away from the porphyroclasts, indicating that the leucosomes have undergone stretching since crystallization (Watt, 1992).

2.2. Younger structures

Minor younger structures are narrow mylonite zones and small scale fracture zones. NW-SE striking mylonitic to ultramylonitic reverse shear zones on the northeastern side of the Mt. Hay block locally cross-cut granulite unit contacts and granulite facies fabrics (Fig. 2). Individual shear zones have N-side-up and S-side-up shear indicators, and slightly different mineral assemblages, suggesting either different periods of uplift or a diachronous conjugate set. In the S-side-up mylonite zones (<10 m wide), a biotite-rich matrix surrounds porphyroclasts of pyroxene, quartz, feldspar, and garnet. Alteration of pyroxene to hornblende, hornblende to red-brown biotite, and garnet to biotite occurs adjacent to the mylonite zones and decreases away from the mylonite within <10 m perpendicular to strike. Lenses of the unaltered intermediate granulite (1–3 m thick and <15 m parallel to strike) are preserved within the mylonite zones. Meter-scale lenses of quartzite and rare garnet quartzite, lying sub-parallel to the foliation, also occur next to and within the mylonite zones. The mineral assemblages in the mylonite and the retrogression in adjacent granulites indicate deformation in the mylonite zones occurred at amphibolite facies. Teyssier (1985) also documented a S-side-up amphibolite facies shear zone (~650 °C, 6 kb) east of Capricorn ridge (Amburla Dam area), which we correlate with those exposed on Capricorn ridge. Exposures of N-side-up mylonite zones are <3 m wide. These mylonites contain chlorite and are associated with minor deformed pegmatites. Minor cataclastic deformation near and within the mylonite zones is recorded by fractures containing pseudotachylite and ultracataclasite. The presence of <3 m thick fracture zones are inferred from the local abundance of fracturing in granulite outcrops and from topographic and map patterns (Fig. 2). Traces of these fracture zones both parallel the mylonite zones, and intersect the zones at high angles. Our mapping indicates the lower crustal structures in Capricorn ridge can be reconstructed despite the effects of these small-scale mylonitic and cataclastic deformation zones.

3. Capricorn ridge shear zone

The three major granulite map units in the Capricorn ridge shear zone are anorthositic, pyroxenitic + quartzofeldspathic, and intermediate granulite (Figs. 2 and 3). The general assemblage in the granulites is orthopyroxene + plagioclase + oxide(s) ± clinopyroxene ± quartz ± hornblende, except for the quartzofeldspathic granulite, which contains potassium feldspar + plagioclase + quartz + oxide(s) ± orthopyroxene ± garnet ± biotite. All granulite units are compositionally heterogeneous at the m-scale (Fig. 3). In addition to the association of quartzofeldspathic and pyroxenitic granulite, relative amounts of plagioclase and mafic minerals define more mafic or felsic

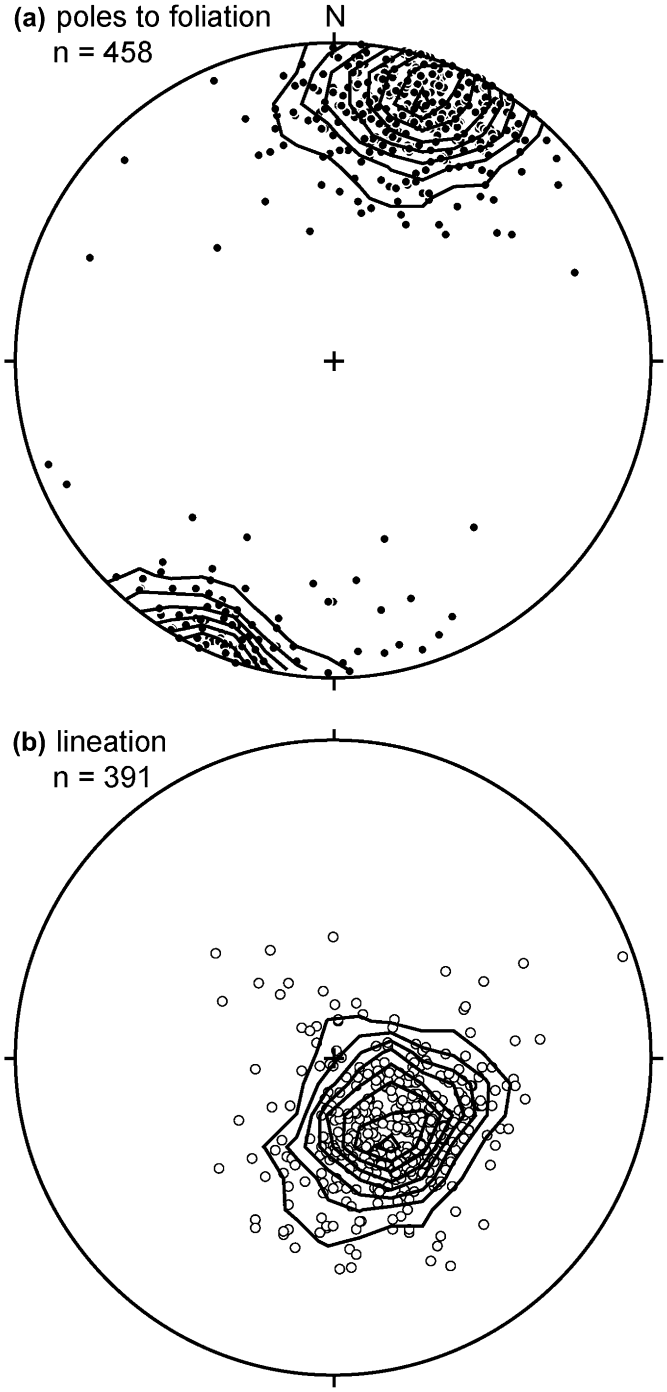

Fig. 4. (a) Poles to foliation; and (b) lineation in granulites in central and western Capricorn ridge (equal area, lower hemisphere projections). Contours are in intervals of 2.0%/1.0% area.

lenses and layers in the anorthositic and intermediate granulite (Figs. 5–7). The intermediate granulite unit contains rare magnetite-rich varieties and magnetite seams.

3.1. Outcrop scale structures

Aligned long axes of mineral grains, trains of mineral grains, and cm-scale compositional domains with flattened-prolate shapes define a penetrative mesoscale lineation. Lineation plunges steeply SSE-SE except where modified by younger structures (Figs. 2 and 4). In addition to the aspect ratio of the lineation, lineation intensity is defined by the degree of dimensional alignment of mineral grains, trains of mineral grains, and quartzofeldspathic stringers. Relative lineation intensity is consistently strongest in quartz ± feldspar-rich domains, weakest in plagioclase-rich domains, and intermediate in pyroxene-rich domains, regardless of the granulite map unit in which they occur (Fig. 3). Quartz ribbons in the quartz ± feldspar domains have aspect ratios up to 10:1. Pyroxene and plagioclase grains in the pyroxenitic and intermediate granulite have aspect ratios $\leq$3:1. Plagioclase grains in the anorthositic granulite have aspect ratios $\leq$2:1. Pyroxene aggregates in the intermediate granulite have aspect ratios up to 8:1. Pyroxene aggregates in the pyroxenitic domains have aspect ratios up to 5:1. The only systematic spatial variation in lineation intensity occurs within quartzofeldspathic domains, as described in Section 4. Lineations in adjacent pyroxenitic and quartzofeldspathic domains are subparallel.

Mesoscale foliation on Capricorn ridge is primarily defined by the alignment of compositional layers and lenses at the cm- to the 100 m-scales, and by cm-scale flattened-prolate mineral aggregates (Figs. 3 and 5–7). We use ''compositional layering'' as a general term referring to the alignment of both layers and lenses. Compositional domain contacts are sharp within the pyroxenitic + quartzofeldspathic unit and sharp to gradational (up to 30 cm perpendicular to the contact) within the other two units. Foliation dips steeply SSW except where modified by younger structures (Figs. 2 and 4). Map patterns indicate that the major lithologic units have tabular shapes with contacts subparallel to the internal foliation (Fig. 2). Foliation intensity varies in Capricorn ridge, which we describe and use below to define across-strike fabric gradients.

Grain shape fabric is parallel to the foliation and lineation defined by the shape of compositional domains. In outcrop, grain shape fabric intensity is consistently strongest in quartz ± feldspar domains, weakest in plagioclase-rich domains, and intermediate in pyroxene-rich domains. Compositional domains predominantly define an S > L fabric in Capricorn ridge, whereas the internal grain shape fabric is generally L > S.

Locally, mesoscale structures in the pyroxenitic + quartzofeldspathic granulite record components of elongation in the foliation plane both perpendicular and parallel to the stretching lineation (Figs. 5, 8 and 9). Extensional shear zones record left-lateral offset when NE-striking and right-lateral offset when NW-striking (Fig. 8). Apparent separation of compositional layers is <10 cm. The extensional shear zones are oblique to the compositional layering by ~20–40°. These structures are interpreted as conjugate shear zones that record ENE-WNW extension, with the line of intersection between the shear zones and foliation subparallel to the lineation. Boudins record extension subparallel to and subperpendicular to the stretching lineation. Axes of tight minor folds plunge shallowly WNW and ESE and parallel to the lineation (Fig. 9b,e,g). Mushroom-shaped (cm- to dm-scale) cross-sections locally indicate the presence of sheath-like folds (Fig. 5c). Overprinting relationships and U-shaped lineation

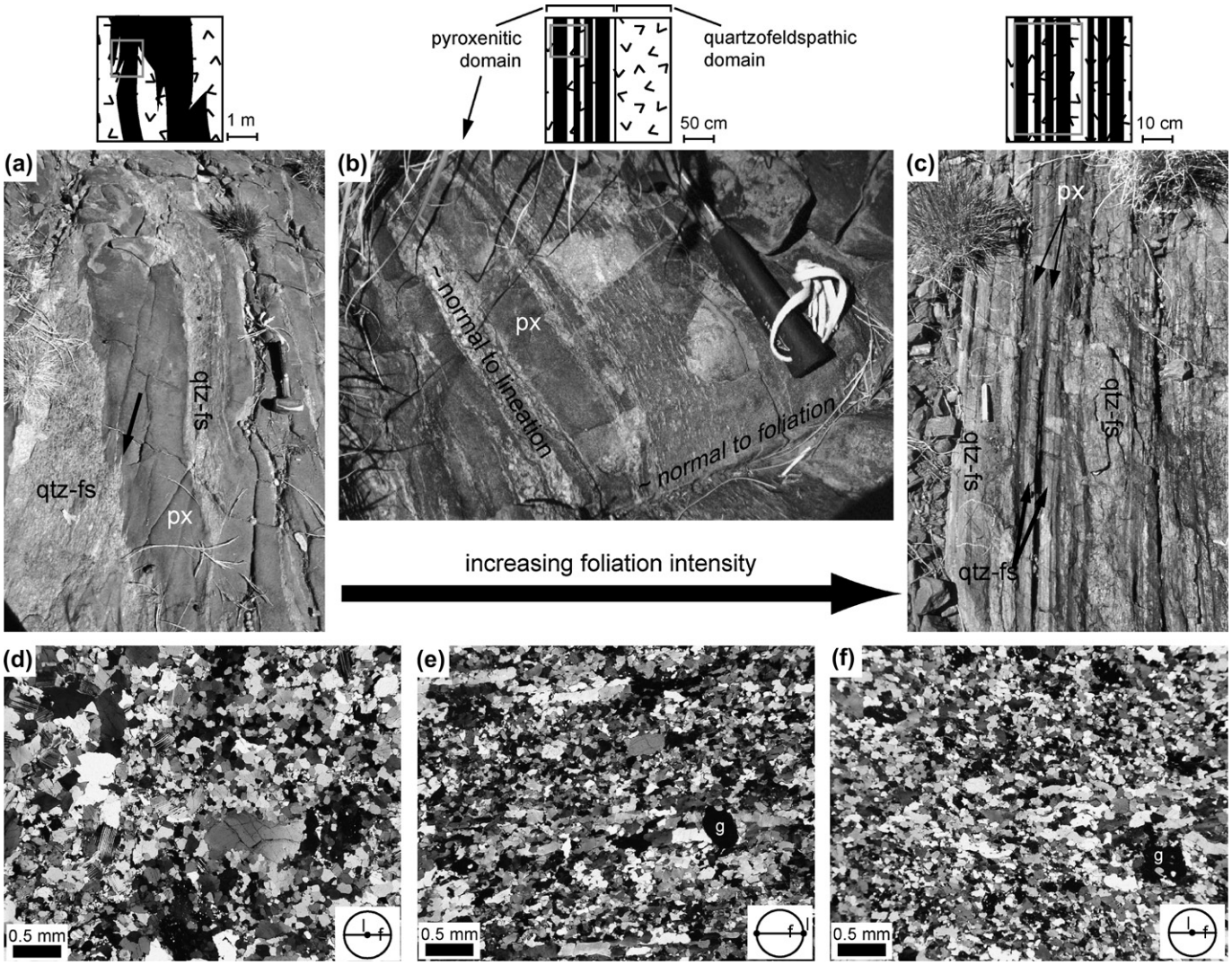

Fig. 5. Outcrop photographs of fabric map units within the pyroxenitic + quartzofeldspathic granulite lithologic map unit (see also Figs. 3 and 11). The large arrow indicates an interpreted increase in foliation intensity. (a–c) Fields of view are oblique to foliation and lineation. (a) Highly cuspate (arrow) compositional domain interfaces between pyroxenitic and quartzofeldspathic domains in the lower fabric intensity unit in Fig. 11. (b) Fabric in a 2 m-thick pyroxenitic layer within the moderate fabric intensity unit. Internal foliation defined by the orientation of flattened-prolate quartzofeldspathic aggregates. (c) Transition between regular m-scale layer thickness to cm-scale thickness (transitional between higher and moderate fabric intensity units). Hammer shown for scale is 27 cm long; pencil in (c) is 12 cm long. Photomicrographs (crossed-polars) of quartzofeldspathic domains in lower (d), moderate (e), and higher (f) fabric intensity. Fields of view with respect to lineation (l) and foliation (f) shown. Photomicrographs show (d) larger grains, wider grain size distribution, and L $\gg$ S fabric defined by grain shape preferred orientation in lower fabric intensity unit in comparison to (f) smaller grains, narrower grain size distribution, and development of LS fabric in higher fabric intensity unit. Larger grains in (d) are feldspars. (e) Photomicrograph of quartz ribbons and S-side-up (dextral as shown) shear sense. Scale indicated by bar. Abbreviations: px, pyroxenitic; qtz-fs, quartzofeldspathic; g, garnet.

patterns suggesting either refolding during progressive deformation or two phases of deformation (e.g., Ramsay, 1980; Ghosh et al., 1999) are not observed, but minor folds are too rare to eliminate the possibility that these are not true sheath folds. As discussed in Section 4, the sheath-like folds only occur in the most strongly foliated zones. Although not observable in three dimensions, it is inferred that the sheath-like folds are elongate subparallel to the stretching lineation in the outcrop.

Mesoscale shear sense indicators are only observed in the pyroxenitic + quartzofeldspathic granulite unit (Figs. 5 and 8). These indicators are asymmetric porphyroclast systems of orthopyroxene, garnet, and feldspar cores and felsic wings with σ- and δ-type geometries. These porphyroclast systems are usually complex, although the most elongate clasts yield the most consistent shear sense, which is S-side-up. Asymmetric feldspar augen with the same shear sense also occur in rare quartzofeldspathic lenses and layers in the intermediate granulite.

3.2. Microstructural observations

Since this study focuses on mesoscale fabric information, microstructural characteristics in the Capricorn ridge granulites are described only to indicate evidence for penetrative ductile deformation. Detailed microstructural work is in progress and will address particular deformation mechanisms and

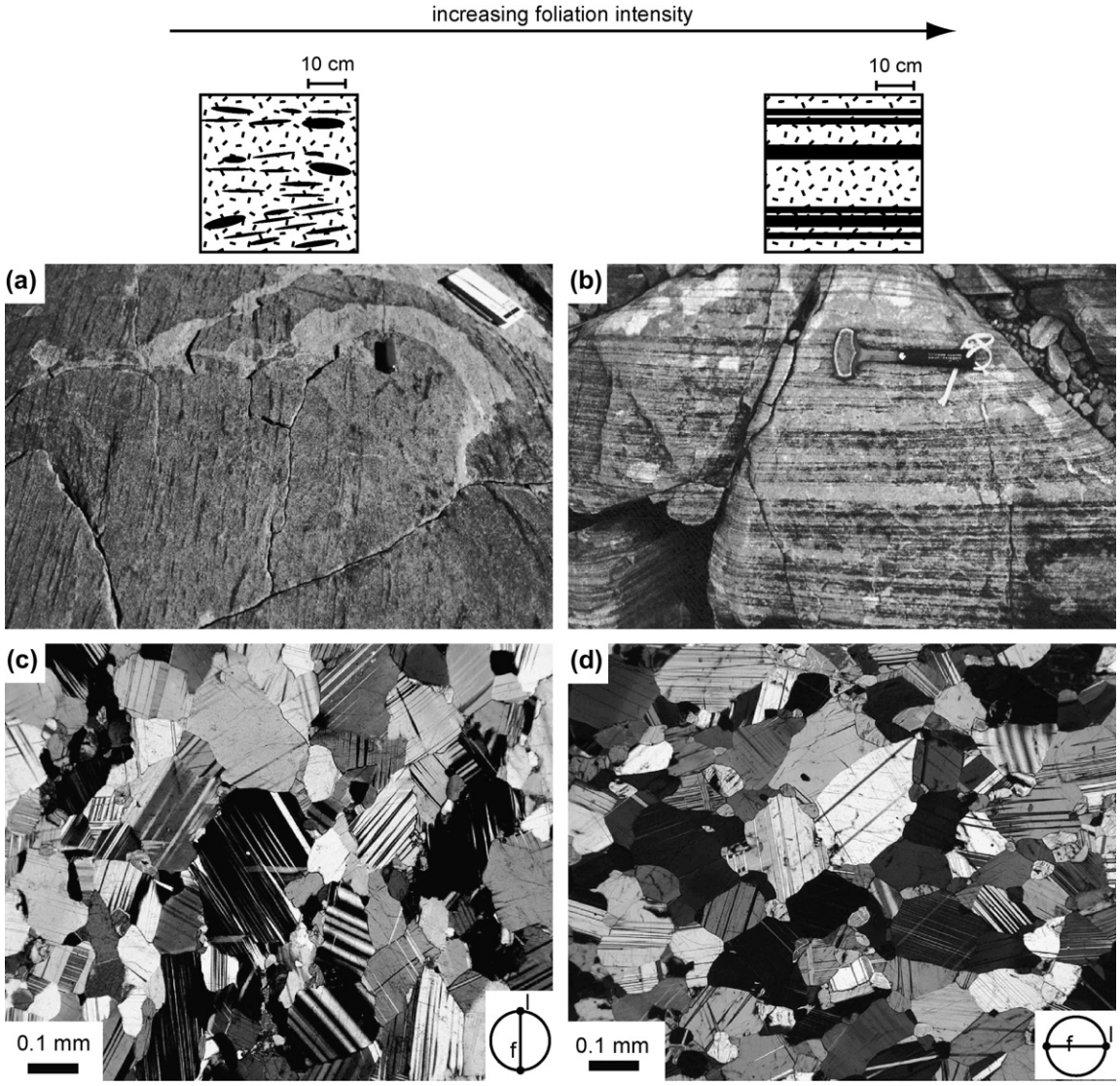

Fig. 6. Outcrop photographs of fabric map units within anorthositic granulite (Fig. 11): (a) Outcrop photograph of discontinuous mafic domains in moderate fabric intensity anorthositic granulite. Penknife is 9 cm long. (b) Outcrop photograph of planar compositional layering of cm-scale thicknesses in higher fabric intensity anorthositic granulite. Hammer shown for scale is 27 cm long. Fields of view are oblique to foliation and sub-perpendicular to lineation. Photomicrographs (crossed-polars) of plagioclase-rich domains in moderate (c) and higher (d) fabric intensity anorthositic granulite. Fields of view with respect to lineation (l) and foliation (f) shown.

lattice preferred orientations, and their significance in the context of the field relationships described here.

Capricorn ridge granulites are characterized microstructurally by evidence of penetrative recrystallization, interlobate to granoblastic grain boundary networks, rare porphyroclasts and rare inclusions. Evidence of intracrystalline strain is observed in all minerals of the granulite facies assemblage (except garnet and oxides). Common microstructures indicative of intracrystalline strain include tapered deformation twins in plagioclase, and undulose extinction in quartz and feldspar and rarely in pyroxene. Plagioclase porphyroclasts exhibit sweeping extinction and deformation twins. Orthopyroxene porphyroclasts exhibit patchy extinction. Rare porphyroclasts in the anorthositic granulite have strongly lobate grain boundaries and abundant inclusions. Primary igneous microstructures and microstructures characteristic of partial melting (e.g., Sawyer, 1999) are not observed (also Glikson, 1984; Teyssier, 1985; Watt, 1992; this study).

Microstructural shear sense indicators in the pyroxenitic + quartzofeldspathic unit are similar to those in outcrop (Fig. 8). Porphyroclasts in the anorthositic granulite do not define a consistent shape fabric, nor are they part of core-and-mantle or mantle structures (Passchier and Trouw, 1996), and thus do not define any fabric asymmetry. Preliminary lattice preferred orientation measurements suggest that plagioclase in the anorthositic granulite and quartz in the quartzofeldspathic granulite have random to weak orientations (Waters-Tormey, 2004).

Microstructures in plagioclase and quartz are consistent with deformation at upper amphibolite to granulite facies conditions. In the quartzofeldspathic granulite, subgrain and grain boundaries within quartz ribbons are perpendicular to the long axes of the ribbons, which is characteristic of high grade

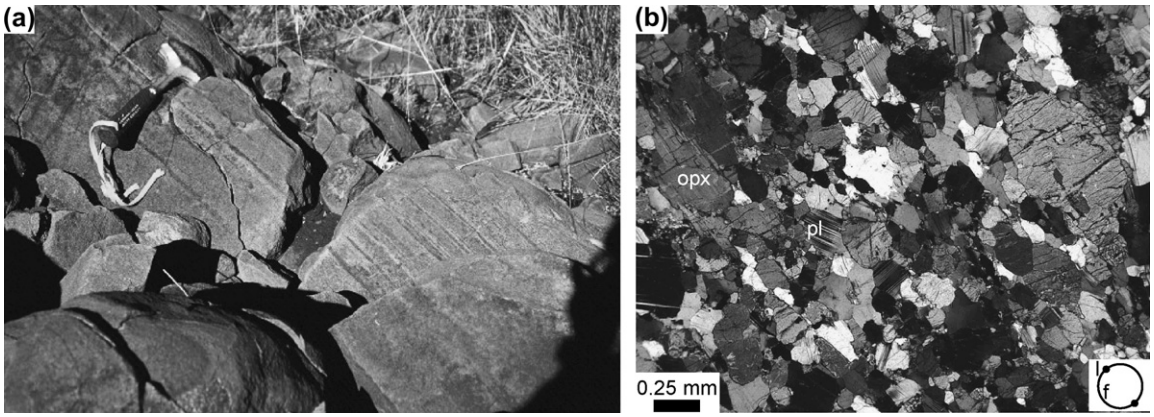

Fig. 7. (a) Outcrop photograph showing compositional layering in moderate fabric intensity intermediate granulite. Hammer shown for scale is 27 cm long. Field of view is perpendicular to foliation and oblique to lineation. (b) Photomicrograph from pyroxene-rich domain in intermediate granulite (crossed-polars). Field of view in photomicrographs is parallel to lineation (l) and perpendicular to foliation (f). Abbreviations: pl, plagioclase; opx, orthopyroxene.

(>600 °C) tectonites (type B3 of Boullier and Bouchez, 1978; Mainprice et al., 1986; Okudaira et al., 1995). In the anorthositic granulite, straight to interlobate boundaries and 120° triple junctions are common between plagioclase grains. Phase boundaries are generally sharp and straight to gently curved. Plagioclase grains are not compositionally zoned (Watt, 1992; this study). The overall microstructural character for the anorthositic granulite is similar to that described for anorthosite deformed at temperatures >700 °C (e.g., LaFrance et al., 1995).

Grain size varies with lithology. The anorthositic granulite has the coarsest grain size overall, with plagioclase grains ~0.1 mm and mafic minerals 0.1–3 mm in their longest dimensions. Pyroxene and plagioclase grains in the intermediate granulite are ~0.2 mm in their longest dimensions. Pyroxene grains in the pyroxenitic granulite are ~0.03 mm in their longest dimensions. The only systematic variation in overall grain size (from ~0.2–0.5 mm) occurs within quartzofeldspathic domains, as described in Section 4.

3.3. Compositional layering is a secondary structure

The lithologic domains in Capricorn ridge likely have a primary origin; lithologic contacts may reflect primary igneous layering or intrusive surfaces (e.g., Bonnay et al., 2000). However, field and microstructural observations indicate that the present compositional layering in Capricorn ridge is a secondary structure. Lithologic contacts at all scales are generally subparallel to each other, and are subparallel to foliation defined by grain shape (Figs. 4 and 9). The only exceptions are rare cuspate contacts between compositional domains in the least well-foliated pyroxenitic + quartzofeldspathic granulite (Fig. 5). The cusps are subparallel to the overall compositional layering and the grain shape foliation. These cusps could be mullions resulting from competency contrast during deformation either in a solid or migmatitic state (Talbot and Sokoutis, 1992), or could have formed during intrusion (Bonnay et al., 2000) and then were rotated into sub-parallelism during deformation. In this and the other granulite units, an increase in the parallelism and planarity of contacts is associated with increasing fabric intensity within compositional layers and lenses (Section 4). Together, these and the above observations indicate that the present compositional layering is not stromatic migmatite layering (e.g., Sawyer, 2001), nor the result of syntectonic magmatic layering (e.g., Lucas and St. Onge, 1995), nor sill-like mutual intrusion (e.g., Bonnay et al., 2000). Instead, the layering is a secondary transposition foliation developed during progressive deformation.

3.4. Constraints on local kinematics of deformation

Meso- and microscale structures suggest that deformation in the Capricorn ridge granulites involved components of flattening and simple shear (Fig. 8f). A penetrative stretching lineation records the maximum finite stretch direction (subparallel to the X kinematic axis). Conjugate extensional shear zones indicate stretching in the foliation plane and perpendicular to lineation, and record elongation subperpendicular to the maximum finite stretch direction (subparallel to the Y kinematic axis). Consistent shear sense indicators are only observed on faces that are perpendicular to the foliation and parallel to the lineation (i.e., XZ kinematic plane). As described below, the overall fabric type on Capricorn ridge is $S > L$. Further, a component of shortening perpendicular to the shear plane, in addition to the possibility of heterogeneous deformation at the scale of observation (Fig. 8b) and complex rotation patterns of non-rigid, flattened-prolate clasts, could explain the complex shear sense indicators observed on Capricorn ridge (Ghosh and Ramberg, 1976; Passchier and Simpson, 1986; Simpson and DePaor, 1993).

3.5. Summary

Outcrop and microstructural observations indicate that Capricorn ridge is a km-scale, penetratively deformed zone in which foliations and lineations are subparallel throughout. Mesoscale structures indicate components of flattening and

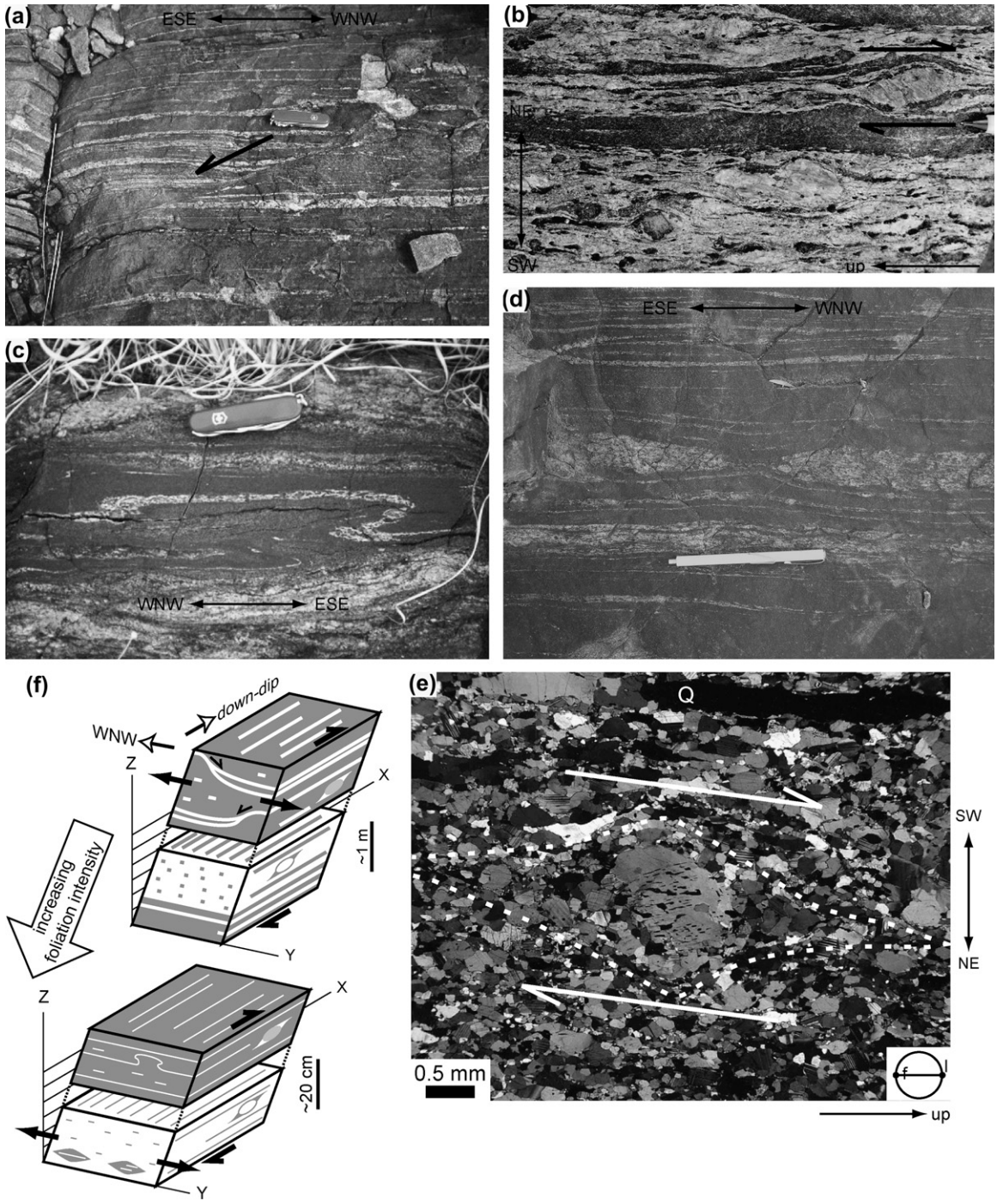

Fig. 8. Outcrop photographs of mesoscale structures within the pyroxenitic + quartzofeldspathic granulite: (a) extensional shear band trace, (b) shear sense indicators and (d) boudins of quartzofeldspathic layer in moderate fabric intensity unit; (c) cross-section of sheath-like fold in higher fabric intensity unit; (d). The outcrop surfaces in (a, c, d) are subperpendicular to foliation and highly oblique to lineation. The outcrop surface in (b) is subparallel to lineation and perpendicular to foliation. Scale: (a, c) Penknife is 9 cm long; (d) magnet is 15 cm long. (e) Photomicrograph from pyroxenitic domain in moderate fabric intensity unit (Fig. 5b). Asymmetric porphyroclast system, slightly oblique to foliation at this scale, indicates S-side-up (shape indicated by white dashed line). Highly elongate quartz grains in upper part of photograph (Q). (f) Illustration of the interpretation of fabric and mesoscale structures in mafic + felsic granulite on Capricorn ridge (mafic = dark gray; felsic = white). Conjugate extensional shear zones and boudins record a component of widening parallel to the Y kinematic axis. The deformation is widening-thinning-lengthening. Shear is parallel to the X axis in the XZ plane. Foliation is shown as horizontal.

S-side-up shear during one progressive deformation. Microstructural characteristics, overall grain size, and lineation intensity depend upon lithology and do not vary systematically across strike in Capricorn ridge.

4. Fabric intensity variation

Relative fabric intensity can indicate relative finite strain intensity even when strain markers are lacking (e.g., Cobbold and

Gapais, 1987; Hanmer, 1987; Passchier et al., 1990; Passchier and Trouw, 1996). In km-scale deformed zones such as those exposed in the Mt. Hay block, a map of relative fabric intensity is the only way to characterize larger scale strain heterogeneity. Within Capricorn ridge, intensity of compositional layering is the only mesoscopic fabric element that varies systematically. The only exception is the variation in grain size and relative lineation intensity in the volumetrically minor quartzofeldspathic domains. Interestingly, these observations contrast with many ductile shear zones where mesoscale fabric intensity is expressed by across-strike penetrative grain size reduction and/or progressive rotation of foliation.

4.1. Variation in mesoscale foliation characteristics

Overall, compositional domains become thinner, more tabular, continuous, and parallel gradationally across strike. These characteristics are used to define 2–3 relative foliation intensity types (lower, moderate and higher). ''Lower'' is used instead of ''low'', etc., to emphasize that these are *relative* intensities within a penetratively deformed zone. Foliation intensity characteristics do not correlate exactly between lithologic units, which is attributable to the nature of the protoliths and how deformation affected them. For this reason, fabric intensity variations in each lithologic map unit are described separately below.

4.2. Fabric gradient in pyroxenitic + quartzofeldspathic granulite

4.2.1. Lower fabric intensity

In the middle of the pyroxenitic + quartzofeldspathic unit, quartzofeldspathic domains have lenticular shapes with m-scale foliation-perpendicular thicknesses and foliation-parallel aspect ratios less than 5:1 (Fig. 5a). They are enclosed by pyroxenitic domains. Contacts between the pyroxenitic and quartzofeldspathic domains are irregular to strongly cuspate. Within the pyroxenitic domains, mm- to cm-scale pyroxene and quartz ± feldspar aggregates have flattened-prolate shapes that define L (lineation only) to L > S fabrics. Larger quartzofeldspathic domains have an internal S > L (foliation better developed than lineation) augen gneissic fabric with potassium feldspar and orthopyroxene porphyroclasts up to 2 cm in longest dimension, and surrounding quartz + feldspar aggregates averaging ~0.5 mm. Foliations in adjacent pyroxenitic and larger quartzofeldspathic domains are oblique by <20° to one another, but are overall parallel to the rest of Capricorn ridge (Figs. 9e and 10a). Rare tight mesoscale fold axes are parallel to lineation (Fig. 9e).

4.2.2. Moderate fabric intensity

Outwards across strike from the middle of the pyroxenitic + quartzofeldspathic unit towards the major lithologic contacts to the NE and SW, compositional domains gradually become thinner and more tabular in shape, and foliation within the domains becomes more parallel and regularly spaced (Fig. 5b). The pyroxenitic and larger quartzofeldspathic domains form layers or lenses with m-scale thicknesses and aspect ratios >10:1 (observed perpendicular to lineation and foliation). Compositional domain boundaries are increasingly more planar and parallel. Within quartzofeldspathic domains, most grains are ~0.2 mm in longest dimension, grain size distributions are more uniform (Fig. 5e), and a stronger L > S fabric develops. Garnet grains have aspect ratios up to 3:1 parallel to lineation. Within the pyroxenitic layers, cm-scale quartzofeldspathic layers and lenses define an S > L fabric (Fig. 5b). In a given outcrop, foliation strikes within m-scale quartzofeldspathic layers are often rotated clockwise by 10–15° with respect to that within adjacent pyroxenitic layers, but are overall parallel to the rest of Capricorn ridge (Figs. 9e and 10b,c). Conjugate extensional shear zones and boudinage also occur in this fabric intensity zone (Fig. 8). Rare tight mesoscale fold axes plunge both NW and parallel to lineation (Fig. 9b,g).

4.2.3. Higher fabric intensity

Near the margins of the pyroxenitic + quartzofeldspathic unit, compositional domains are arranged in a regular, planar layering with cm-scale layer thicknesses (Fig. 5c). Quartzofeldspathic layers have a uniform grain size distribution with a grain size that is similar to that in the moderate fabric intensity (~0.2 mm). Quartzofeldspathic layers have a penetrative LS fabric partly defined at the microscale by quartz ribbons with aspect ratios up to 10:1. Locally, pyroxenitic layers contain thinner, tabular quartzofeldspathic layers and lenses that define an S > L fabric. Where measurable, foliation within adjacent compositional layers is parallel (Fig. 10d). The decrease from m-scale to cm-scale thicknesses in this higher fabric intensity zone represents thinning by at least an order of magnitude.

Rare boudinage on faces subperpendicular to lineation, and sheath-like folds, also occur in this fabric intensity zone, whereas conjugate extensional shear zones do not. Rare tight mesoscale fold axes plunge both NW and parallel to lineation (Fig. 9b,g).

4.3. Fabric gradient in anorthositic granulite

The across-strike fabric intensity gradient in the anorthositic granulite is defined by increasing along-strike continuity of layers and lenses (Fig. 6). In the middle of the anorthositic granulite, flattened-prolate mafic aggregates define a compositional layering (Fig. 6a). This foliation type is the lowest relative foliation intensity within the anorthositic granulite, which corresponds to moderate foliation intensity in Capricorn ridge overall. Outwards across strike over several m, the mafic domains increase in lateral continuity. Towards the margins, the foliation is defined by planar felsic and mafic layers with thicknesses on the order of cm (Fig. 6b). This foliation type corresponds with higher foliation intensity in Capricorn ridge overall.

4.4. Fabric gradient in intermediate granulite

Map patterns in the intermediate granulite are complicated by the younger thrust faults. Intermediate granulite in southeastern Capricorn ridge is not assigned a fabric intensity due to the prevalence of fracturing and thrust faulting.

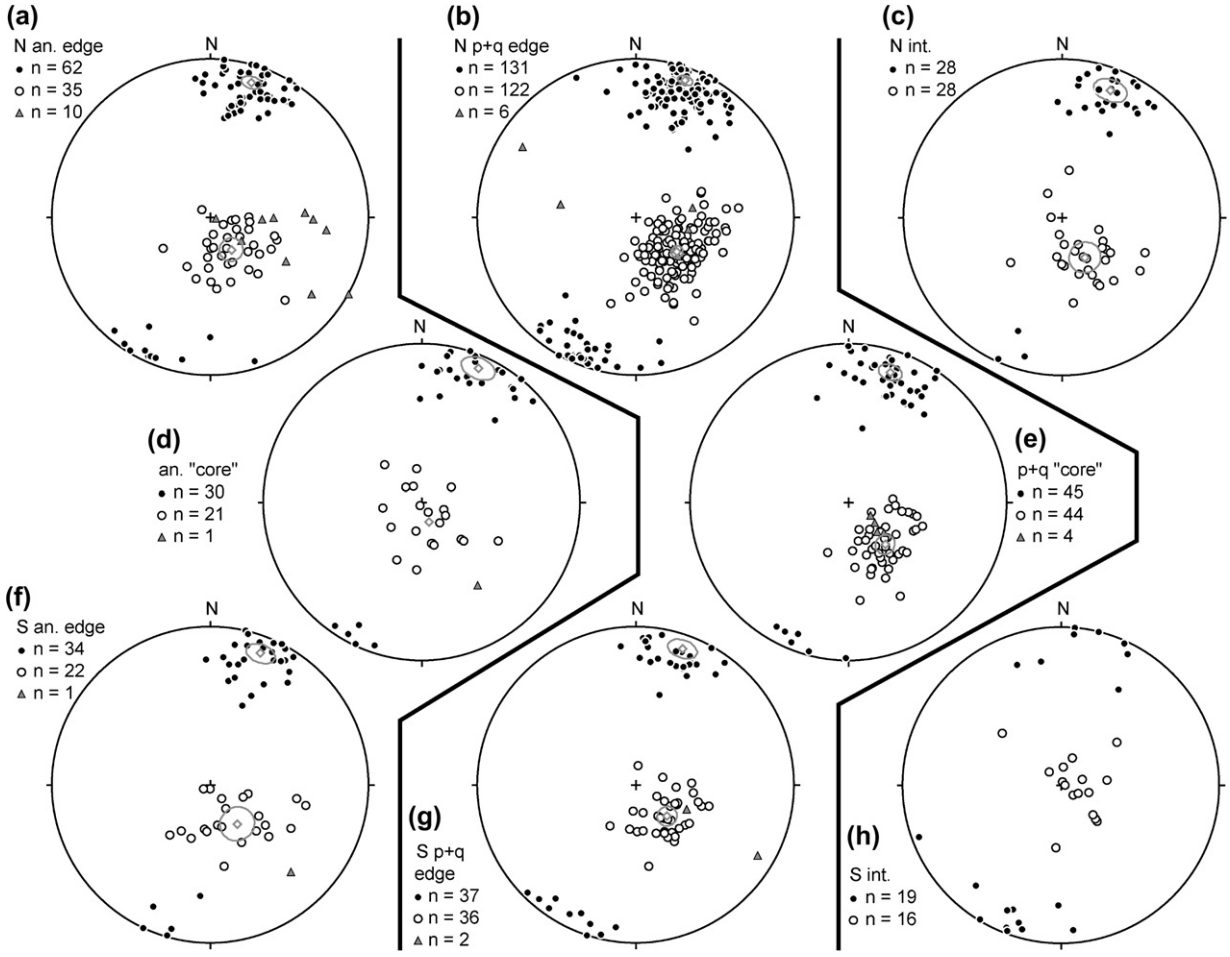

Fig. 9. The orientation of lineation and foliation does not vary significantly across strike within each major lithologic unit. Poles to foliation (filled circles), lineation (open circles), and fold hinges (triangles) are separated spatially into ''cores'' and NE and SW sides, of each major lithologic unit (equal area, lower hemisphere projections). Abbreviations: an., anorthositic granulite; px + q, pyroxenitic + quartzofeldspathic granulite; int., intermediate granulite. (a, f) Higher foliation intensity in the anorthositic granulite. (b, g) Moderate and higher foliation intensities, combined, in the pyroxenitic + quartzofeldspathic granulite. (c) Moderate and higher foliation intensities, combined, in the intermediate granulite. (e, h) Lower foliation intensities in the pyroxenitic + quartzofeldspathic and intermediate granulites, respectively. (d) Moderate foliation intensity zone in the anorthositic granulite. The spatial distribution of foliation intensities is shown in 1. 11. 95% confidence cones for maximum Bingham axial distribution eigenvalues (diamonds) are shown as gray ellipses.

North of the southernmost thrust, three foliation characteristics vary systematically across strike from SW to NE: 1) Foliation orientation becomes more parallel (Figs. 2 and 9h,c); 2) Compositional domain shape grades from L > S to S > L; and 3) Compositional domains develop regular, cm-scale thicknesses (Fig. 7a). These fabric variations can be used to define relative foliation intensity in the intermediate granulite. Lower foliation intensity is defined by irregular compositional domain thickness, varying foliation orientation, and/or L > S fabrics. Moderate foliation intensity is defined by compositional layering that is more parallel across strike and SL fabrics. The higher foliation intensity is defined by parallel compositional layers with thicknesses on the order of cm defining S > L fabrics.

4.5. Correlation between lithologic units to make a fabric map

Even though the foliation intensity gradients in the pyroxenitic + quartzofeldspathic, anorthositic, and intermediate granulites vary in detail, there are significant similarities between them. In all three lithologic units, higher foliation intensity is characterized by tabular, parallel, and laterally continuous compositional layers. Higher foliation intensity zones grade into moderate foliation intensity zones where compositional domains are less tabular, less parallel, and less continuous. Within each unit, the orientation of the foliation and lineation, microstructural characteristics and lineation intensity do not vary significantly across the fabric intensity gradients (Figs. 9 and 10).

These observations suggest that the characteristics used to define relative fabric intensity domains in each lithologic unit can be correlated as ''fabric units''. We note that fabric intensities within one lithologic unit are unlikely to represent identical fabrics or identical fabric intensities in another lithologic unit. In other words, ''moderate'' fabric intensity in the pyroxenitic + quartzofeldspathic granulite does not represent the same amount of fabric development as ''moderate'' fabric intensity in the intermediate granulite.

Fig. 11a is a fabric map of the area shown in Fig. 2. This map shows that, in each lithologic unit, foliation is highest

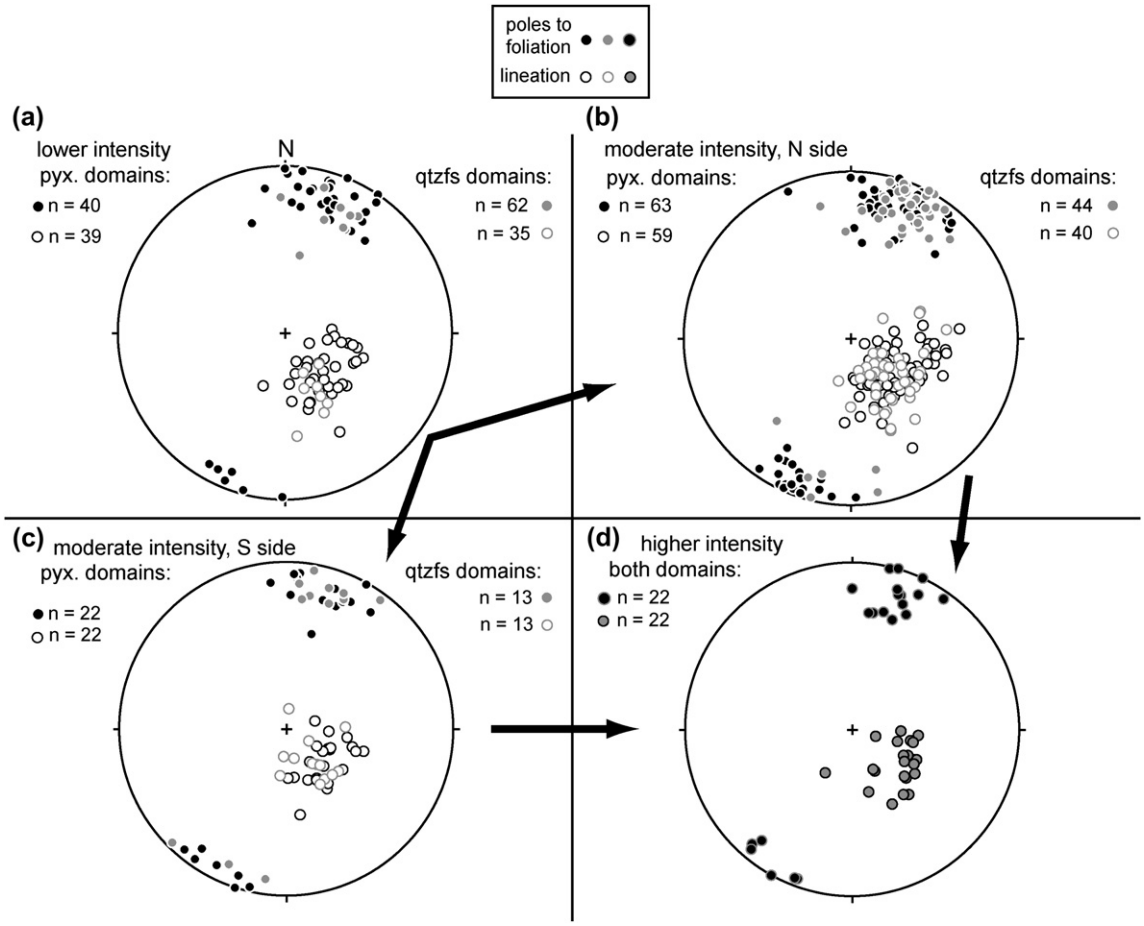

Fig. 10. Equal area, lower hemisphere projections of poles to foliation and lineation within compositional domains of the pyroxenitic + quartzofeldspathic granulite (Figs. 2 and 3). Data are separated out by compositional domain to show that orientations of foliation and lineation in compositional domains do not change between foliation intensity zones. Arrows indicate gradient from lower outwards across strike to higher fabric intensity. The spatial extent of foliation intensity zones is shown in Fig. 11. (a) Lower foliation intensity zone (cf. Fig. 9e). (b, c) Moderate foliation intensity zones on the northern (cf. Fig. 9b) and southern edges (cf. Fig. 9g), respectively. (d) Higher foliation intensity zone (cf. Fig. 9b,g).

in intensity near the contacts with another lithologic unit. This relation is consistent along strike. Contacts between the major lithologic units are gradational over several m and no fault-like discontinuity is observed. These relationships suggest that fabric development was continuous across lithologic margins and that fabric development concentrated at these margins.

5. Discussion

5.1. Inferring relative strain intensity from fabric intensity

Given the absence of finite strain markers and undeformed protoliths in the Capricorn Ridge shear zone, finite strain analysis is not viable. Instead, relative fabric intensity can provide qualitative information about finite strain intensity. In general, increasing finite strain within ductile shear zones is associated with increasing rotation, planarity, lateral continuity, across-strike parallelism, and decreasing thickness of primary lithologic domains (e.g., Myers, 1978, 1997; Grocott and Watterson, 1980; Hanmer, 1984; Davidson, 1984; Simpson, 1985; White and Flagler, 1991; Smit and Van Reenen, 1997; Molli et al., 2000). At the highest strain, primary lithologic domains are thinnest, and contacts are planar and transposed into parallelism with grain shape fabrics (Hobbs et al., 1976). In lower grade ductile shear zones, such progressive secondary compositional foliation development has been corroborated by finite strain analysis (e.g., Ramsay and Graham, 1970; Burg et al., 1981) and is typically accompanied by progressive grain size reduction (e.g., Christie, 1960; Johnson, 1967; Law et al., 1984). Rare strain markers in high grade terranes also corroborate similar progressive intensifying of compositional foliation in shear zones (e.g., Escher et al., 1975; Hanmer et al., 1994; Moser, 1994; Srivastava et al., 1995; Myers, 1997).

Several observations indicate that relative foliation intensity represents real variations in strain in Capricorn ridge. First, the across-strike variation in relative foliation intensity in each lithologic unit is systematic. Second, the transition from one type of foliation intensity to the next is similar to increasing foliation intensity gradients documented in other shear zones. This transition is especially marked in the

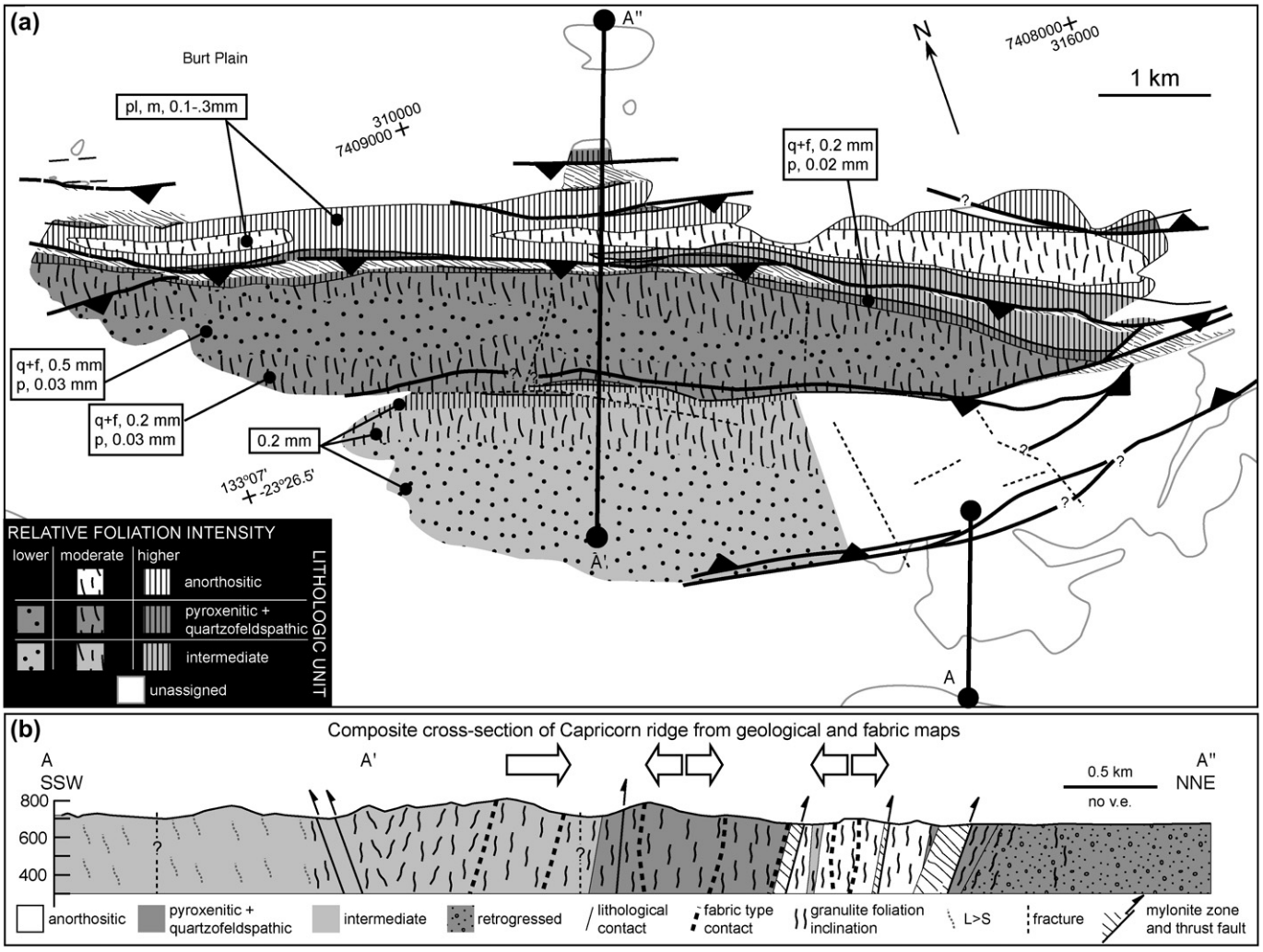

Fig. 11. (a) Fabric map of Capricorn ridge, adapted from Fig. 2. Shading and contacts as in Fig. 2; relative compositional layering intensity shown in patterns. The absence of patterns or shading indicates unassigned fabric intensity in areas of overprinting. Fabric unit contacts are transitional over several m. (b) Composite cross-section of Capricorn ridge after geological map (Fig. 2) and fabric map (part a). Fabric contacts are indicated within each lithologic unit. Large arrows show direction of increasing foliation intensity towards major lithologic boundaries. Cross-section traces shown on Fig. 2 and in part (a). No vertical exaggeration.

pyroxenitic + quartzofeldspathic unit, where increasing planarity, lateral continuity, and across-strike parallelism of compositional domains are accompanied by a significant reduction in lithologic domain thickness from m- to cm-scale (Fig. 5). Mesoscale structures also indicate that foliation intensity is related to finite strain as sheath-like folds only occur in the highest fabric intensity zone. The higher foliation intensity units in both the intermediate and anorthositic granulites share similar foliation intensity characteristics, despite having different protoliths. Third, the progression of increasingly oblate fabric types with increasing finite strain is consistent with deformations involving a combination of flattening and simple shear (Fossen and Tikoff, 1998).

The fabric gradients in the anorthositic and intermediate granulite units are not straightforward to interpret in terms of progressive deformation. It is possible that the foliation intensity characteristics in these units are the result of primary geological heterogeneities not present in the other units. However, the change in foliation characteristics described for the anorthositic and intermediate granulites, such as increasing planarity, are still consistent with increasing finite strain. Further, if strain magnitude is continuous across the lithologic transitions, as suggested by the physical continuity across the contacts, relative fabric development should be similar in the different lithologic units juxtaposed along the contacts.

Progressive grain size reduction only occurs in the quartzofeldspathic domains, despite evidence for finite strain variation inferred from relative fabric intensity for all compositional domains. Intracrystalline strain and overall non-equilibrium grain boundary microstructures indicate that these granulites are recrystallized but that extensive static recrystallization is not responsible for the observed grain size distributions (cf., Vernon, 1968).

5.2. *Evidence that Capricorn ridge is a high strain shear zone*

A comparison between Capricorn and Mt. Hay ridges also indicates that Capricorn ridge is a high strain shear zone (Waters-Tormey et al., *in review*). Primary igneous fabrics

are not observed on Capricorn ridge, although they occur locally on Mt. Hay (Bonnay et al., 2000). Pyroxenitic and quartzofeldspathic domains in Capricorn ridge are thinner and more tabular, and have straighter boundaries than those in the same unit on Mt. Hay ridge. Evidence for transposition on Capricorn ridge, such as the parallelism of primary lithologic contacts and grain shape fabric, does not occur on Mt. Hay ridge. Additionally, quartzofeldspathic augen gneiss is often medium to coarse-grained on Mt. Hay ridge (also Bonnay et al., 2000), whereas similar quartzofeldspathic augen gneiss is rare on Capricorn ridge. If the coarser-grained gneiss is the protolith for both augen gneisses, this is evidence that these bodies have undergone more deformation on Capricorn ridge. Last, sheath-like folds are locally associated with the higher fabric intensity zones on Capricorn ridge. The transposition of primary features and sheath folds both indicate high shear strains (typically $\gamma > 10$; Cobbold and Quinquis, 1980; Hobbs et al., 1976; Vollmer, 1988). All of these observations indicate that Capricorn ridge is a high strain shear zone.

5.3. Strain localization within Capricorn ridge

The fabric map developed from compositional layering intensity observations allows us to make inferences about strain patterns in Capricorn ridge at the 100-m- to km-scales. The highest relative fabric intensity in each major lithologic unit occurs near their boundaries. This fabric intensity pattern is interpreted to record strain localization adjacent to the major lithologic boundaries during lower crustal deformation.

Fig. 12 is a simple illustration of how relative fabric intensity is used to infer strain localization. Shading indicates relative fabric intensity and relative strain intensity. The exact magnitude of finite strain is unknown and thus the model is qualitative. Even if the fabric gradients in the anorthositic and intermediate granulites are more a function of primary lithologic heterogeneity rather than of finite strain magnitude, the highest strain in Capricorn ridge (in the pyroxenitic + quartzofeldspathic unit) still occurs adjacent to the major lithologic contacts.

We have therefore interpreted lower crustal strain localization at two scales in the Mt. Hay block. The first scale is that of Capricorn ridge itself, which is interpreted as a >6 km thick high strain zone. Within this high strain zone, additional strain localization occurs with 100 m-scale spacings, and is adjacent to the major lithologic contacts.

5.4. Strain gradients across lithologic boundaries and competency contrast

The major finding from our study is that finite strain is concentrated at major lithologic boundaries on Capricorn ridge. Strain localization at lithologic domain interfaces indicates attachment between two domains with different competencies (e.g., Sengupta, 1997). Field observations of meso- and macroscale shear strain localization adjacent to lithologic domain interfaces have been documented elsewhere (Escher et al., 1975; Talbot, 1982; Hanmer, 1984; Nadeau and Hanmer, 1992; Sengupta, 1997). In these studies, strain localization at lithologic interfaces is recorded by one of two strain patterns: 1) Foliation orientation that is sigmoidal across to the interface; or 2) Fabric intensity that is highest adjacent to the interface.

Existing theoretical considerations and physical modeling indicate that strain localization adjacent to infinite competency domain interfaces requires components of shear and shortening perpendicular to the shear plane (Ghosh and Ramberg, 1976; Treagus and Sokoutis, 1992; Sengupta, 1997). Strain patterns in adjacent incompetent and competent layers in two types of two-dimensional deformations are shown in Fig. 13. Domain interfaces are parallel to the shear plane. In Fig. 13a,b, deformation involved components of layer-parallel shear and layer-perpendicular shortening. The highest strain occurs adjacent to the interface. When deformation does not include a component of shortening perpendicular to the shear plane, finite strain refraction patterns result instead and the highest strain develops in the least competent layer (Fig. 13c; e.g., Treagus, 1983). These models are applicable to naturally deformed rocks such as those in Capricorn ridge, as competency domains with aspect ratios as low as 3:1 have been shown to act like infinite layers in terms of strain localization (Ghosh and Ramberg, 1976; Sengupta, 1997).

The location and degree of strain localization also depend on the configuration of competency domains in the system. During deformation, the steepest interface-perpendicular strain gradient forms when the interface is at a high angle to the bulk maximum shortening direction. In this case, the maximum contrast in mechanical behavior occurs due to a combination of contrast in shear strain, elongation, and rotation rates. In order to maintain a continuous deformation (strain compatibility), strain rate accelerates within an accommodation zone that straddles the interface (Fig. 13a,b). The strain localization patterns (Fig. 11) and kinematic constraints on deformation in Capricorn ridge (Fig. 8) are internally consistent and indicate that strain localized at competency boundaries due to a combination of flattening and simple shear. Even though the bulk sense of shear in Capricorn ridge is somewhat ambiguous, this is the easiest way to explain strain localization adjacent to the lithologic boundaries instead of strain refraction patterns.

One major difference between some of the studies above and our results is that foliation in Capricorn ridge is parallel across the competency boundaries (Fig. 13b). We interpret the difference to result from higher strain recorded in Capricorn ridge. If an earlier sigmoidal pattern was originally present, it has been obliterated by progressive deformation whereas the fabric intensity gradients remained. The orientation of foliation away from the interfaces and the interfaces themselves rotated into subparallelism with the foliation during transposition.

This hypothesis requires that, despite the high homologous temperatures during deformation, competency contrast existed between the major lithologic units. Mesoscale structures recording competency contrast observed in Capricorn ridge, such as boudins and segregation of incompetent domains into mesoscale shear zones, support this hypothesis at a smaller

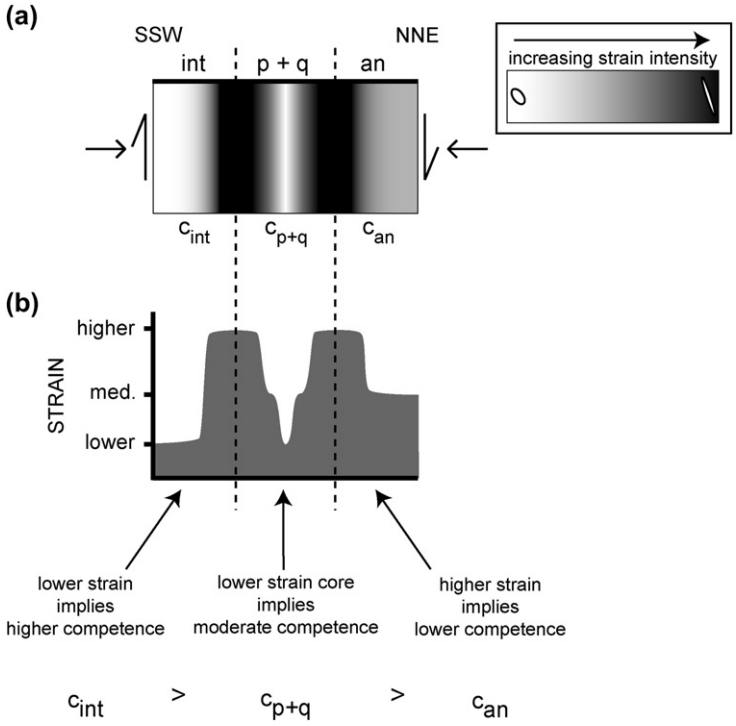

Fig. 12. (a) Schematic cross-sectional view of the major lithologic boundaries (dashed lines) in Capricorn ridge (prior to amphibolite facies thrust faulting). Abbreviations: int (intermediate granulite), p + q (pyroxenitic + quartzofeldspathic granulite), an (anorthositic granulite). (a) Shading indicates relative fabric intensity, which is interpreted as relative strain intensity. (b) Alternative representation of relative strain intensities interpreted from fabric intensity. Strain gradients straddle the major lithologic boundaries. The strain patterns are consistent with competency contrast between the major lithologic units. Relative competency for each lithology, as inferred from the finite strain pattern, is also indicated ($c_{int} > c_{p+q} > c_{an}$).

scale (e.g., Biot, 1965; Platt and Vissers, 1980). At present, we can only speculate about the relative competencies of the compositional domains and lithologic units on Capricorn ridge. At the outcrop scale, the thickness of a particular quartzofeldspathic domain appears to have determined whether it was more or less competent than the adjacent pyroxenitic domains (Fig. 8a,d). If the relative intensity of grain shape fabrics increases with decreasing competency, then the order of least to most competent is: quartz + feldspar-rich, pyroxene-rich, plagioclase-rich. At the km-scale, our classification of relative fabric intensities indicates a progression, in order of least to most competent, of: anorthositic, pyroxenitic + quartzofeldspathic, and intermediate granulite (Figs. 11 and 12). There is, however, no measurable asymmetry in the widths of the strain gradients adjacent to the major lithologic contacts that would corroborate this interpretation (Sengupta, 1997). Finally, it is possible that the variation in composition and/or effective thicknesses resulted in different competency contrasts at different scales.

5.5. Implications for lower crustal deformation

The Mt. Hay area is a particularly good area for characterizing lower-crustal deformation. Lower crustal exposures (e.g., Fountain et al., 1992; Hanmer et al., 1995; Myers, 1997), xenoliths (e.g., Rudnick and Fountain, 1995; Chen et al., 2001), and seismic velocity analyses (e.g., Christensen and Mooney, 1995; Rudnick and Fountain, 1995) indicate that pyroxene- and plagioclase-rich granulites are abundant in the lower continental crust. The Mt. Hay granulites have these lithologies. Second, the granulites in Mt. Hay deformed at temperatures typical for the lower continental crust (>600°). Third, the granulite facies deformation in Capricorn Ridge occurred during one progressive event. The effects of the younger tectonism are distinctive so that there is little ambiguity about the relative timing of overprinting relationships. Finally, the >6 km thickness of the Capricorn ridge high strain zone indicates that it was a major strain localization zone in the lower crust during the (late) Strangways tectonic event.

Within the Capricorn ridge high strain zone, all the lithologic domains were penetratively deformed at granulite facies conditions. Yet, there is evidence for competency contrast between rock types with both relatively small (pyroxenitic and intermediate) and more significant (pyroxenitic and anorthositic) differences in composition. Further, the southern margin of the Capricorn ridge shear zone is not marked by a major change in lithology (still primarily pyroxene + plagioclase). Given the lower continental crust is compositionally heterogeneous in km-scale exposures, and varies in bulk composition regionally, our study suggests that lower continental crust may not be uniformly weak (e.g., Kohlstedt et al., 1995) or uniformly strong (e.g., Jackson, 2002).

The primary manifestation of competency contrast in Capricorn ridge is strain localization at the contacts between major (100 m-scale) lithologic domains. Lithologic heterogeneity at this scale is common in lower crustal exposures, often taking

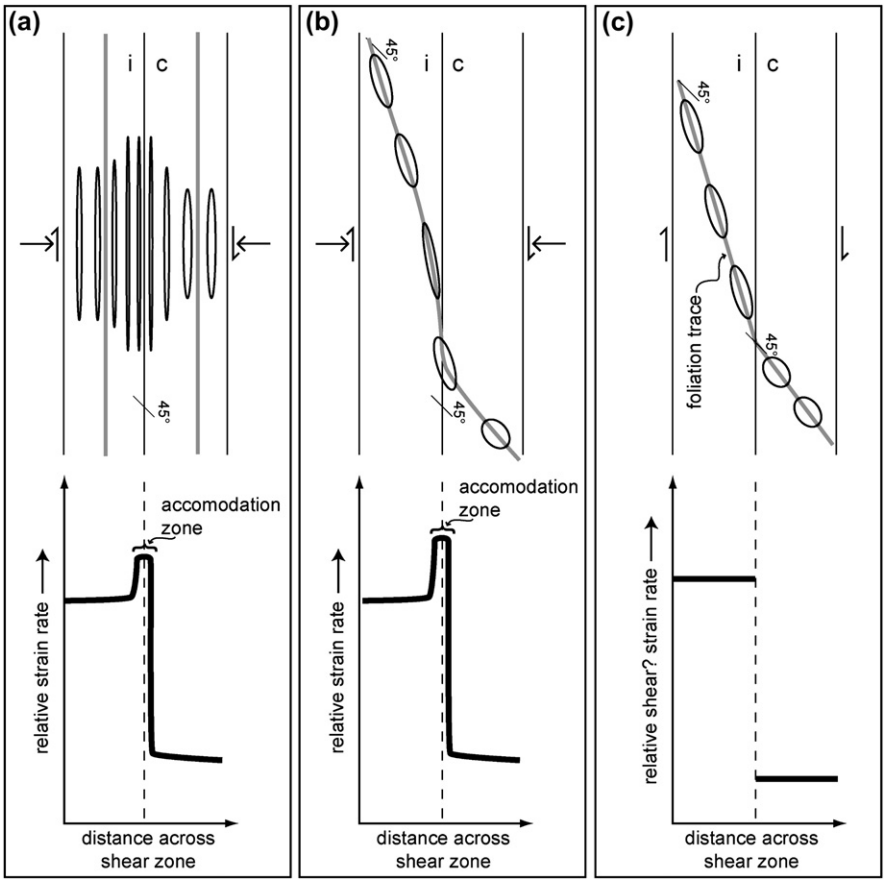

Fig. 13. Schematic illustrations of the effect of competency contrast, deformation kinematics and finite strain on relative strain intensity in a shear zone that contains a competent layer (*c*) and an incompetent layer (*i*). Layer interfaces are attachment surfaces. Deformation involves both pure and simple shear in (a, b); simple shear only in (c). The upper diagram is a cross-section of the shear zone. Gray lines represent foliation traces. The degree of ellipticity indicates relative deformation intensity. Overall finite strain (ellipticity) is higher within relatively incompetent domains. The lower diagrams show the corresponding relative strain rate across the shear zone during deformation. Relative strain rate is due to competency contrast and inferred from relative strain intensity. (a) The foliation orientation (parallel to interface) and relative finite strain magnitude pattern observed in Capricorn ridge. Relative finite strain magnitude changes smoothly across the competency interface. Continuous deformation across the interface requires an accommodation zone within which the strain rate is higher. The strain rate pattern is similar to (b). (b) Shear strain localization adjacent to the layer interface as recorded by a sigmoidal foliation trace and finite strain intensity (after Sengupta, 1997). Foliation orientation and relative finite strain magnitude change smoothly across interface. As in part (a), continuous deformation requires an accommodation zone with a higher strain rate. (c) Foliation refraction example where foliation orientation and relative finite strain magnitude change sharply at the interface. Foliation refraction only occurs in the absence of layer-perpendicular shortening (e.g., Sengupta, 1997).

the form of compositional layering defined by layers or aligned lenses (e.g., Katz, 1969; Annor and Freeth, 1985; Dawson et al., 1986; Gibson and Simpson, 1988; Leclair and Poirier, 1989; Salisbury and Fountain, 1990; Kroner et al., 1994; Percival and West, 1994; Anto et al., 1999; Martelat et al., 1999; Hippertt et al., 2001; Mauler et al., 2001; Zulauf, 2001; Azcarraga et al., 2002; Vassallo and Wilson, 2002). Thus, the particular distribution and arrangement of major lithologic contacts may influence strain localization sites and spacings in the lower crust during ductile deformation. It is interesting to note that the (late) Strangways deformation localized in what, at least now, is the most lithologically heterogeneous part of the Mt. Hay block – Capricorn ridge.

Strain localization adjacent to attachments between competency domains in Capricorn ridge contrasts with most conceptual models for lower crustal deformation, which implicitly or explicitly assume that deformation localizes within weak lithologic phases or fine grained zones. On Capricorn ridge, first order strain localization is not associated with a particular rock type or grain size. It may be that attachments between competency domains in lithologically heterogeneous zones – which are poorly understood as yet – are as important as grain scale processes in terms of the causes of ductile strain localization in the lower crust.

6. Conclusions

Conclusions drawn from this study are:

(1) Capricorn ridge is a >6 km-thick high strain zone that formed in the lower crust during the (late) Strangways tectonic event. The granulites in Capricorn ridge are penetratively recrystallized. Foliation and lineation are parallel throughout the zone. Evidence for high finite strain includes complete transposition of primary geological contacts into the foliation and locally, sheath-like folds.

(2) Deformation in Capricorn ridge seems to have developed during a single progressive deformation because all structures can be placed in the context of a single deformation event involving the combination of flattening and simple shear.
(3) A fabric map illustrates relative across-strike variation in fabric intensity in Capricorn ridge, which is best defined by the intensity of compositional foliation. In general, foliation intensity is highest at major lithologic contacts, with overall grain size not changing significantly with increasing finite strain.
(4) Interpreting the observed fabric gradients in terms of finite strain, we can qualitatively evaluate relative strain intensity within the shear zone. Strain is localized at lithologic boundaries.
(5) The inferred strain gradients indicate that competency contrast can exist between lithologic domains at relatively high homologous temperatures. This interpretation is also supported directly by field observation of structures such as boudinage. The evidence for competency contrast and strain localization is inconsistent with a uniformly strong or uniformly weak mechanical behavior of lithologically heterogeneous lower continental crust.

Acknowledgements

We would like to thank Drs. Laurel Goodwin, Simon Hanmer and Geoffrey Lloyd, and Mr. Daniel Tatham, for their thorough reviews that helped to improve the final manuscript. CWT wishes to thank Christian Teyssier and Paul Kelso for introducing her to this field site. The Northern Territory Geological Survey office in Alice Springs provided invaluable logistical assistance and regional geological knowledge. Christine Edgoose and Martin Cardena are particularly appreciated. The Dann and Evans families generously gave permission for us to work on their property. CWT wishes to especially acknowledge the Danns for their hospitality. Lauren Hewitt, Blair Tormey, and Mark Waters provided assistance in the field. The work was supported by a Packard Foundation grant to BT and National Science Foundation grant EAR-0440156. The Vilas travel and Weeks fund grants (University of Wisconsin) and Sigma Xi provided additional support for CWT.

References

Agar, S.M., 1994. Rheological evolution of the ocean crust; a microstructural view. Journal of Geophysical Research 99, 3175–3200.

Allen, A.R., Stubbs, D., 1982. $An^{40}Ar/^{39}Ar$ study of a polymetamorphic complex in the Arunta Block, central Australia. Contributions to Mineralogy and Petrology 79, 319–332.

Altenberger, U., 1997. Strain localization mechanisms in deep-seated layered rocks. Geologische Rundschau 86, 56–58.

Annor, A.E., Freeth, S.J., 1985. Thermo-tectonic evolution of the basement complex around Okene, Nigeria, with special reference to deformation mechanism. Precambrian Research 28, 269–281.

Anto, K.F., Janardhan, A.S., Basavalingu, B., 1999. Metamorphic history of calc-silicate lithologies from the Kambam Valley, Tamil Nadu, and its bearing on the evolution of the Southern Granulite Terrain. Journal of the Geological Society of India 53, 27–37.

Arbaret, L., Burg, J.P., 2003. Complex flow in lowest crustal, anastomosing mylonites: Strain gradients in a Kohistan gabbro, northern Pakistan. Journal of Geophysical Research 108, 2467.

Austrheim, H., 1987. Eclogitization of lower crustal granulites by fluid migration through shear zones. Earth and Planetary Science Letters 81, 221–232.

Azcarraga, J., Abalos, B., Gil-Ibarguchi, J.I., 2002. On the relationship between kilometer-scale sheath folds, ductile thrusts and minor structures in the basal high-pressure units of the Cabo Ortegal. Journal of Structural Geology 24, 1971–1989.

Ballevre, M., Bastiaan, J.H., Reynard, B., 1997. Orthopyroxene-andalusite symplectites replacing cordierite in granulite from the Strangways Range (Arunta Block, central Australia): a new twist to the pressure-temperature history. Geology 25, 215–218.

Behrmann, J.H., Mainprice, D., 1987. Deformation mechanisms in a high-temperature quartz-feldspar mylonite: evidence for superplastic flow in the lower continental crust. Tectonophysics 140, 297–305.

Benes, V., Davy, P., 1996. Modes of continental lithospheric extension; experimental verification of strain localization processes. Tectonophysics 254, 69–87.

Berthé, D., Choukroune, P., Jegouzo, P., 1979. Orthogneiss, mylonite and non-coaxial deformation of granites: the example of the South Amoricain shear zone. Journal of Structural Geology 1, 31–42.

Biermeier, C., Stüwe, K., Foster, D.A., Finger, F., 2003. Thermal evolution of the Redbank thrust system, central Australia: geochronological and phase-equilibrium constraints. Tectonics 22, 1–23.

Biot, M.A., 1965. Mechanics of Incremental Deformations: Theory of Elasticity and Viscoelasticity of Initially Stressed Solids and Fluids, Including Thermodynamic Foundations and Applications to Finite Strain. Wiley, New York.

Bonnay, M., 2001. Felsic characterization and transfer of the magmas in the average crust to deep, Example: The Hay Mount in central Australia (translated title). Ph.D. thesis, University of Quebec at Chicoutimi.

Bonnay, M., Collins, W.J., Sawyer, E.W., Wiebe, R.A., 2000. Introduction to the Arunta Inlier. In: Collins, W.J. (Ed.), Granite Magma Segregation and Transfer During Compressional Deformation in the Deep Crust? Proterozoic Arunta Inlier, Central Australia, Field Trip Guide FA4. Geological Society of Australia Incorporated, Canberra, pp. 8–46.

Boullier, A.M., Bouchez, J.L., 1978. Quartz ribbons in mylonites. Bulletin de la Societé Geologique de France 7, 253–262.

Brown, M., Solar, G.S., 1998. Shear zone systems and melts: feedback relations and self-organization in orogenic belts. Journal of Structural Geology 20, 211–227.

Burg, J.P., 1999. Ductile structures and instabilities; their implication for Variscan tectonics in the Ardennes. Tectonophysics 309, 1–25.

Burg, J.P., Iglesias, M., Laurent, P., Matte, P., Ribeiro, A., 1981. Variscan intracontinental deformation; the Coimbra-Cordoba shear zone (SW Iberian Peninsula). Tectonophysics 78, 161–177.

Carter, N.L., Tsenn, M.C., 1987. Flow properties of continental lithosphere. Tectonophysics 136, 27–63.

Chen, S., O'Reilly, S.Y., Zhou, X., Griffin, W.L., Zhang, G., Sun, M., Feng, J., Zhang, M., 2001. Thermal and petrological structure of the lithosphere beneath Hannuoba, Sino-Korean Craton, China; evidence from xenoliths. Lithos 56, 267–301.

Chester, F.M., Logan, J.M., 1986. Implications for mechanical properties of brittle faults from observations of the Punchbowl fault zone, California. Pure and Applied Geophysics 124, 79–106.

Christensen, N.I., Mooney, W.D., 1995. Seismic velocity structure and composition of the continental crust: a global view. Journal of Geophysical Research 100, 9761–9788.

Christie, J.M., 1960. Mylonitic rocks of the Moine thrust zone in the Assynt Region, north-west Scotland. Transactions of the Edinburgh Geological Society 18, 79–93.

Claoue-Long, J.C., Hoatson, D.M., 2005. Proterozoic mafic-ultramafic intrusions in the Arunta Region, central Australia Part 2: event chronology and regional correlations. Precambrian Research 142, 134–158.

Cobbold, P.R., Gapais, D., 1987. Shear criteria in rocks: an introductory review. Journal of Structural Geology 9, 521–523.

Cobbold, P.R., Quinquis, H., 1980. Development of sheath folds in shear regimes. Journal of Structural Geology 2, 119–126.

Collins, W.J., Shaw, R.D., 1995. Geochronological constraints on orogenic events in the Arunta Inlier: a review. Precambrian Research 71, 315–346.

Collins, W.J., Teyssier, C., 1989. Crustal scale ductile fault systems in the Arunta Inlier, central Australia. Tectonophysics 158, 49–66.

Crider, J.G., Peacock, D.C.P., 2004. Initiation of brittle faults in the upper crust: a review of field observations. Journal of Structural Geology 26, 691–707.

Davidson, A., 1984. Identification of ductile shear zones in the southwestern Grenville Province of the Canadian Shield. In: Kroener, A., Greiling, R. (Eds.), Precambrian Tectonics Illustrated. E. Schweizerbart'sche Verlagsbuchhandl (Naegele u. Obermiller), Stuttgart, Germany, pp. 263–279.

Dawson, J.B., Carswell, D.A., Hall, J., Wedepohl, K.H. (Eds.), 1986. The Nature of the Lower Continental Crust. Geological Society Special Publications, 24.

Drury, M.R., Vissers, R.L.M., Van-der-Wal, D., Hoogerduijn, S.E.H., 1991. Shear localisation in upper mantle peridotites. Pure and Applied Geophysics 137, 439–460.

Dunlap, W.J., Teyssier, C., 1995. Paleozoic deformation and isotopic disturbance in the southeastern Arunta Block, central Australia. Precambrian Research 71, 229–250.

Dunlap, W.J., Hirth, G., Teyssier, C., 1997. Thermomechanical evolution of a ductile duplex. Tectonics 16, 983–1000.

Dutruge, G., Burg, J.P., 1997. Strain localisation in an orthogneiss laccolith (the Pinet Massif, Aveyron, southern France). Tectonophysics 280, 47–60.

Escher, A., Escher, J.C., Watterson, J., 1975. The reorientation of the Kangamiut dyke swarm, West Greenland. Canadian Journal of Earth Science 12, 158–173.

Evans, J.P., 1988. Deformation mechanisms in granitic rocks at shallow crustal levels. Journal of Structural Geology 10, 437–443.

Fossen, H., Tikoff, B., 1998. Extended models of transpression and transtension, and application to tectonic setting. In: Holdsworth, R.E., Strachan, R.A., Dewey, J.F. (Eds.), Continental Transpressional and Transtensional Tectonics. Geological Society, London, Special Publications, vol. 135, pp. 15–33.

Fountain, D.M., Arculus, R., Kay, R.W. (Eds.), 1992. Continental Lower Crust. Elsevier, Amsterdam.

Gapais, D., Bale, P., Choukroune, P., Cobbold, P.R., Mahjoub, Y., Marquer, D., 1987. Bulk kinematics from shear zone patterns; some field examples. Journal of Structural Geology 9, 635–646.

Gartrell, A.P., 2001. Crustal rheology and its effect on rift basin styles. Geological Society of America Memoir 193, 221–233.

Ghosh, S.K., Hazra, S., Sengupta, 1999. Planar, non-planar and refolded sheath folds in the Phulad Shear Zone, Rajasthan, India. Journal of Structural Geology 21, 1715–1729.

Ghosh, S.K., Ramberg, H., 1976. Reorientation of inclusions by combination of pure shear and simple shear. Tectonophysics 34, 1–70.

Ghosh, S.K., Sengupta, S., 1987. Progressive development of structures in a ductile shear zone. Journal of Structural Geology 9, 277–287.

Gibson, R.G., Simpson, C., 1988. Proterozoic polydeformation in basement rocks of the Needle Mtns., CO. Geological Society of America Bulletin 100, 1957–1970.

Glikson, A.Y., 1984. Granulite-gneiss terranes of the southwestern Arunta Block, central Australia: Glen Helen, Narwietooma, and Anburla 1:100,000 sheet areas. Bureau of Mineral Resources, Australia. Record 1984, 22.

Goleby, B.R., Kennett, B.L.N., Wright, C., Shaw, R.D., Lambeck, K., 1990. Seismic reflection profiling in the Proterozoic Arunta Block, central Australia: processing for testing models of tectonic evolution. Tectonophysics 173, 257–268.

Goodwin, L.B., Wenk, H.R., 1995. Development of phyllonite from granodiorite: mechanisms of grain-size reduction in the Santa Rosa mylonite zone, California. Journal of Structural Geology 17, 689–707.

Grocott, J., Watterson, J., 1980. Strain profile of a boundary within a large ductile shear zone. Journal of Structural Geology 2, 111–117.

Handy, M.R., 1994. Flow laws for rocks containing two non-linear viscous phases: a phenomenological approach. Journal of Structural Geology 16, 278–301.

Handy, M.R., Stunitz, H., 2002. Strain localization by fracturing and reaction weakening: a mechanism for initiating exhumation of subcontinental mantle beneath rifted margins. In: de-Meer, S., Drury, M.R., Martyn, R., de Bresser, J.H.P., Pennock, G.M. (Eds.), Deformation Mechanisms, Rheology and Tectonics; Current Status and Future Perspectives. Geological Society, London, Special Publications, vol. 200, pp. 387–407.

Hanmer, S.K., 1984. Structure of the junction of three tectonic slices: Ontario gneiss segment, Grenville Province. Geological Survey of Canada paper 84-1B, 109–120.

Hanmer, S., 1987. Textural map units in quartzo-feldspathic mylonitic rocks. Canadian Journal of Earth Sciences 24, 2065–2073.

Hanmer, S., 1997. Shear zone reactivation at granulite facies: the importance of plutons in the localization of viscous flow. Journal of the Geological Society of London 154, 111–116.

Hanmer, S., Parrish, R., Williams, M., Kopf, C., 1994. Striding-Athabasca mylonite zone: complex Archean deep-crustal deformation in the east Athabasca mylonite triangle, northern Saskatchewan. Canadian Journal of Earth Science 31, 1287–1300.

Hanmer, S., Williams, M., Kopf, C., 1995. Striding-Athabasca mylonite zone: implications for the Archean and Early Proterozoic tectonics of the western Canadian Shield. Canadian Journal of Earth Sciences 32, 178–196.

Hippertt, J., Rocha, A., Lana, C., Egydio-Silva, M., Takeshita, T., 2001. Quartz plastic segregation and ribbon development in high-grade striped gneisses. Journal of Structural Geology 23, 67–80.

Hoatson, D.M., Claoué-Long, J.C., Shensu, S., 2005. Proterozoic mafic-ultramafic intrusions in the Arunta Region, central Australia Part 1: geological setting and mineral potential. Precambrian Research 142, 93–133.

Hobbs, B.E., Means, W.D., Williams, P.F., 1976. An Outline of Structural Geology. Wiley, New York, 571 pp.

Jackson, J., 2002. Strength of the continental lithosphere; time to abandon the jelly sandwich? Geological Society of America Today 12, 4–10.

Jaroslow, G.E., Hirth, G., Dick, H.J.B., 1996. Abyssal peridotite mylonites; implications for grain-size sensitive flow and strain localization in the oceanic lithosphere. Tectonophysics 256, 17–37.

Jin, D., Karato, S.-I., Obata, M., 1998. Mechanisms of shear localization in the continental lithosphere: inference from the deformation microstructures of peridotites from the Ivrea zone, northwestern Italy. Journal of Structural Geology 20, 195–209.

Johnson, M.R.W., 1967. Mylonite zones and mylonite banding. Nature 213, 246–247.

Katz, M.B., 1969. The nature and origin of the granulites of Mont Tremblant Park, Quebec. Geological Society of America Bulletin 80, 2019–2037.

Kohlstedt, D.L., Evans, B., Mackwell, S.J., 1995. Strength of the lithosphere: constraints imposed by laboratory experiments. Journal of Geophysical Research 100, 17587–17602.

Korsch, R.J., Goleby, B.R., Leven, J.H., Drummond, B.J., 1998. Crustal architecture of central Australia based on deep seismic reflection profiling. Tectonophysics 288, 57–69.

Kroner, A., Kehelpannala, K.V.W., Kriegsman, L.M., 1994. Origin of compositional layering and mechanism of crustal thickening in the high-grade gneiss terrain of Sri Lanka. Precambrian Research 66, 21–37.

Kruse, R., Stunitz, H., 1999. Deformation mechanisms and phase distribution in mafic high-temperature mylonites from the Jotun Nappe, Southern Norway. Tectonophysics 303, 223–249.

LaFrance, B., Clarke, G.L., Collins, W.J., Williams, I.S., 1995. The emplacement of the Wuluma granite: melt generation and migration along steeply dipping extensional fractures at the close of the Late Strangways orogenic event, Arunta Block, central Australia. Precambrian Research 72, 43–67.

Law, R.D., Knipe, R.J., Dayan, H., 1984. Strain path partitioning within thrust sheets; microstructural and petrofabric evidence from the Moine thrust zone at Loch Eriboll, Northwest Scotland. Journal of Structural Geology 6, 477–497.

Leclair, A.D., Poirier, G.G., 1989. The Kapuskasing uplift in the Kapuskasing area, Ontario. Current Research Part C Canadian Shield 89-1C, 225–234.

Lister, G.S., Dornsiepen, U.F., 1982. Fabric transitions in the Saxony granulite gneiss terrane. Journal of Structural Geology 4, 81–92.

Lloyd, G.E., Knipe, R.J., 1992. Deformation mechanisms accommodating faulting of quartzite under upper crustal conditions. Journal of Structural Geology 2, 127–143.

Lloyd, G.E., Mainprice, D., Wheeler, J., 1992. Microstructural and crystal fabric evolution during shear zone formation. Journal of Structural Geology 14, 1079–1100.

Lonka, H., Schulmann, K., Venera, Z., 1998. Ductile deformation of tonalite in the Suomusjarvi shear zone, south-western Finland. Journal of Structural Geology 20, 783–798.

Lucas, S.B., St. Onge, M.R., 1995. Syn-tectonic magmatism and the development of compositional layering, Ungava Orogen (northern Quebec, Canada). Journal of Structural Geology 17, 475–491.

Mainprice, D., Bouchez, J.L., Blumenfeld, P., Tubia, J.M., 1986. Dominant c slip in naturally deformed quartz: implications for dramatic plastic softening at high temperature. Geology 14, 819–822.

Martelat, J.M., Schulmann, K., Lardeaux, J.M., Nicollet, C., Cardon, H., 1999. Granulite microfabrics and deformation mechanisms in southern Madagascar. Journal of Structural Geology 21, 671–687.

Mauler, A., Godard, G., Kunze, K., 2001. Crystallographic fabrics of omphacite, rutile and quartz in Vendee eclogites (Armorican Massif, France): consequences for deformation mechanisms and regimes. Tectonophysics 342, 81–112.

Miller, E.L., Gans, P.B., Garing, J., 1983. The Snake Range decollement; an exhumed mid-Tertiary ductile-brittle transition. Tectonics 2, 239–263.

Molli, G., Conti, P., Giorgetti, G., Meccheri, M., Oesterling, N., 2000. Microfabric study on the deformational and thermal history of the Alpi Apuane marbles (Carrara marbles), Italy. Journal of Structural Geology 22, 1809–1825.

Molnar, P., 1992. Brace-Goetz strength profiles, the partitioning and strike-slip and thrust faulting at zones of oblique convergence, and the stress-heat flow paradox of the San Andreas fault. In: Evans, B., Wong, T.F. (Eds.), Fault Mechanics and Transport Properties of Rocks. Academic, San Diego, California, pp. 359–435.

Moser, D.E., 1994. The geology and structure of the mid-crustal Wawa gneiss domain: a key to understanding tectonic variation with depth and time in the late Archean Abitibi-Wawa Orogen. Canadian Journal of Earth Science 31, 1064–1080.

Myers, J.S., 1978. Formation of banded gneisses by deformation of igneous rocks. Precambrian Research 6, 43–64.

Myers, J.S., 1997. Tectonic evolution of deep crustal structures in the mid-Proterozoic Albany-Fraser orogen, western Australia. In: Sengupta, S. (Ed.), Evolution of Geological Structures in Micro- to Macro-scales. Chapman and Hall, London, pp. 473–485.

Myers, J.S., Shaw, R.D., Tyler, I.M., 1996. Tectonic evolution of Proterozoic Australia. Tectonics 15, 1431–1446.

Nadeau, L., Hanmer, S., 1992. Deep-crustal break-back stacking and slow exhumation of the continental footwall beneath a thrusted marginal basin, Grenville orogen, Canada. Tectonophysics 210, 215–233.

Newman, J., Lamb, W.M., Drury, M.R., Vissers, R.L.M., 1999. Deformation processes in a peridotite shear zone: reaction-softening by an H_2O-deficient, continuous net transfer reaction. Tectonophysics 303, 193–222.

Okudaira, T., Takeshita, T., Hara, I., Ando, J., 1995. A new estimate of the conditions for transition from basal ⟨a⟩ to prism [c] slip in naturally deformed quartz. Tectonophysics 250, 31–46.

Olgaard, D.L., 1990. The role of second phase in localizing deformation. In: Knipe, R.J., Rutter, E.H. (Eds.), Deformation Mechanisms, Rheology and Tectonics. Geological Society Special Publications, 54, pp. 175–181.

Passchier, C.W., Simpson, C., 1986. Porphyroclast systems as kinematic indicators. Journal of Structural Geology 8, 831–843.

Passchier, C.W., Trouw, R.A.J., 1996. Microtectonics. Springer, New York.

Passchier, C.W., Myers, J.S., Kroner, A., 1990. Field Geology of High-Grade Gneiss Terranes. Springer, New York.

Paterson, M.S., 1995. A theory for granular flow accommodated by material transfer via an intergranular fluid. Tectonophysics 245, 135–151.

Percival, J.A., West, G., 1994. The Kapuskasing Uplift; a geological and geophysical synthesis. Canadian Journal of Earth Science 31, 1256–1286.

Platt, J.P., Vissers, R.L.M., 1980. Extensional structures in anisotropic rocks. Journal of Structural Geology 2, 397–410.

Ramsay, J.G., Graham, R.H., 1970. Strain variation in shear belts. Canadian Journal of Earth Science 7, 786–873.

Ramsay, J.G., 1980. Shear zone geometry: a review. Journal of Structural Geology 2, 83–99.

Rosenberg, C.L., Stunitz, H., 2003. Deformation and rxlln of plagioclase along a temperature gradient: an example from the Bergell tonalite. Journal of Structural Geology 25, 389–408.

Rudnick, R.L., Fountain, D.M., 1995. Nature and composition of the continental crust: a lower crustal perspective. Reviews of Geophysics 33, 267–309.

Rutter, E.H., 1999. On the relationship between the formation of shear zones and the form of the flow law for rocks undergoing dynamic recrystallization. Tectonophysics 303, 147–158.

Salisbury, M.H., Fountain, D.M., (Eds.), 1990. Exposed Cross-Sections of the Continental Crust. NATO ASI Series, Series C: Mathematical and Physical Sciences 317.

Sawyer, E.W., 1999. Criteria for the recognition of partial melting. Physics and Chemistry of the Earth 24, 269–279.

Sawyer, E.W., 2001. Grain-scale and outcrop-scale distribution and movement of melt in a crystallising granite. Geological Society of America Special Paper 350, 73–85.

Scholz, C.H., 1988. The brittle-plastic transition and the depth of seismic faulting. Geologische Rundschau 77, 319–328.

Sengupta, S., 1997. Contrasting fabrics in deformed dikes and host rocks: natural examples and a simplified model. In: Sengupta, S. (Ed.), Evolution of Geological Structures in Micro- to Macro-scales. Chapman and Hall, London, pp. 341–372.

Shaw, R.D., Black, L.P., 1991. The history and tectonic implications of the Redbank Thrust Zone, central Australia, based on structural, metamorphic and Rb-Sr isotopic evidence. Australian Journal of Earth Science 38, 307–332.

Shaw, R.D., Stewart, A.J., Black, L.P., 1984. The Arunta Inlier: a complex ensialic mobile belt in central Australia, Part 2: tectonic history. Australian Journal of Earth Sciences 31, 457–484.

Shaw, R.D., Etheridge, M.A., Lambeck, K., 1991. Development of the late Proterozoic to mid-Paleozoic intracratonic Amadeus basin in central Australia: a key to understanding tectonic forces in plate interiors. Tectonics 10, 688–721.

Simpson, C., 1985. Deformation of granitic rocks across the brittle-ductile transition. Journal of Structural Geology 7, 503–511.

Simpson, C., DePaor, D., 1993. Strain and kinematic analysis in shear zones. Journal of Structural Geology 15, 1–20.

Smit, C.A., Van Reenen, D.D., 1997. Deep crustal shear zones, high-grade tectonites, and associated metasomatic alteration in the Limpopo Belt, South Africa: implications for deep crustal processes. Journal of Geology 105, 37–57.

Snoke, A.W., Kalakay, T.J., Quick, J.E., Sinigoi, S., 1999. Development of a deep-crustal shear zone in response to syntectonic intrusion of mafic magma into the lower crust, Ivrea-Verbano zone, Italy. Earth and Planetary Science Letters 166, 31–45.

Srivastava, H.B., Hudleston, P., Earley III, D., 1995. Strain and possible volume loss in a high-grade ductile shear zone. Journal of Structural Geology 17, 1217–1231.

Stipp, M., Stunitz, H., Heilbronner, R., Schmid, S.M., 2002. The eastern Tonale fault zone: a 'natural laboratory' for crystal-plastic deformation of quartz over a temperature range of 250–700 °C. Journal of Structural Geology 24, 1861–1884.

Talbot, C.J., 1982. Obliquely foliated dikes as deformed incompetent single layers. Geological Society of America Bulletin 93, 450–460.

Talbot, C.J., Sokoutis, D., 1992. The importance of incompetence. Geology 20, 951–953.

Teyssier, C., 1985. High strain zones in the continental crust the central Australian example. Ph.D. Thesis, Monash University.

Teyssier, C., Amri, C., Hobbs, B.E., 1988. Southern Arunta Block: the internal zones of a Proterozoic overthrust in central Australia. Precambrian Research 40-41, 157–173.

Tikoff, B., Goodwin, L., 2002. Competency contrast, kinematics, and the development of foliations and lineations in the crust. Journal of Structural Geology 24, 1065–1085.

Treagus, S.H., 1983. A theory of finite strain variation through contrasting layers, and its bearing on cleavage refraction. Journal of Structural Geology 5, 351–368.

Treagus, S.H., Sokoutis, D., 1992. Laboratory modeling of strain variation across rheological boundaries. Journal of Structural Geology 14, 405–424.

Tsurumi, J., Hosonuma, H., Kanagawa, K., 2003. Strain localization due to a positive feedback of deformation and myrmekite-forming reaction in granite and aplite mylonites along the Hatagawa shear zone of NE Japan. Journal of Structural Geology 25, 557–574.

Van der Hilst, R.D., Kennett, B.L.N., Shibutani, T., 1998. Lithospheric and mantle structure beneath Australia. In: Braun, J. (Ed.), Structure and Evolution of the Australian Continent. Geodynamics Series, 26. American Geophysical Union, Washington, D.C, pp. 39–57.

Vassallo, J.J., Wilson, C.J.L., 2002. Palaeoproterozoic regional-scale non-coaxial deformation: an example from eastern Eyre peninsula, South Australia. Journal of Structural Geology 24, 1–24.

Vernon, R.H., 1968. Microstructures of high-grade metamorphic rocks at Broken Hill, Australia. Journal of Petrology 9, 1–22.

Vissers, R.L.M., Drury, M.R., Newman, J., Fliervoet, T.F., 1997. Mylonitic deformation in upper mantle peridotites of the North Pyrenean Zone (France); implications for strength and strain localization in the lithosphere. Tectonophysics 279, 303–325.

Vollmer, F.W., 1988. A computer model of sheath-nappes formed during crustal shear in the Western Gneiss Region, central Norwiegan Caledonides. Journal of Structural Geology 10, 735–743.

Warren, R.G., Shaw, R.D., 1995. Hermmansburg, Northern Territory 1:250,000 Geological Series. Bureau Mineral Resources of Australia Explanatory Notes SF/53 and Map.

Waters-Tormey, C., 2004. Structural Geology of a ten kilometer scale lower crustal shear zone: Mt. Hay granulites, central Australia. Ph.D. thesis, University of Wisconsin at Madison.

Waters-Tormey, C., Staffier, K., Tikoff, B., Goodwin, L., Kelso, P., A granulite-facies, normal shear zone exposed in Mt. Hay block, Arunta block, central Australia: implications for lower crustal deformation during oblique divergence. Geological Society of America Special Publication, *in review*.

Watt, G., 1992. Geology of the Mount Hay – Mount Chapple massif (Arunta Block, Hermannsburg 1:250,000 Sheet area, central Australia): field report, 1990. Bureau Mineral Resources of Australia, Record 1992/22.

Watts, M.J., Williams, G.D., 1983. Strain geometry, microstructure and mineral chemistry in metagabbro shear zones: a study of softening mechanisms during progressive mylonitization. Journal of Structural Geology 5, 507–517.

Wellman, P., 1988. Development of the Australian Proterozoic crust as inferred from gravity and magnetic anomalies. Precambrian Research 40-41, 89–100.

White, S.H., Bretan, P.G., 1985. Rheological controls on the geometry of deep faults and the tectonic delamination of the continental crust. Tectonics 4, 303–309.

White, J.C., Flagler, P.A., 1991. Deformation within part of a major crustal shear zone, Parry Sound, Ontario: structure and kinematics. Canadian Journal of Earth Science 29, 129–141.

Whitmeyer, S.J., Simpson, C., 2003. High strain-rate deformation fabrics characterize a kilometers-thick Paleozoic fault zone in the eastern Sierras Pampeanas, central Argentina. Journal of Structural Geology 25, 909–922.

Williams, M.L., Melis, E.A., Kopf, C.F., Hanmer, S., 2000. Microstructural tectonometamorphic processes and the development of gneissic layering: a mechanism for metamorphic segretation. Journal of Metamorphic Geology 18, 41–57.

Young, D.N., Fanning, C.M., Shaw, R.D., Edgoose, C.J., Blake, D.H., Page, R.W., Camacho, A., 1995. U-Pb zircon dating of tectonomagmatic events in the northern Arunta Inlier, central Australia. Precambrian Research 71, 45–68.

Zhao, J., Bennett, V.C., 1995. SHRIMP U-Pb zircon geochronology of granites in the Arunta Inlier, central Australia: implications for Proterozoic crustal evolution. Precambrian Research 71, 17–43.

Zhao, J.X., McCulloch, 1995. Geochemical and Nd isotopic systematics of granites from the Arunta Inlier, central Australia: implications for Proterozoic crustal evolution. Precambrian Research 71, 265–299.

Zulauf, G., 2001. Structural style, deformation mechanisms and paleodifferential stress along an exposed crustal section; constraints on the rheology of quartzofeldspathic rocks at supra- and infrastructural levels (Bohemian Massif). Tectonophysics 332, 211–237.